Mapping the safe operating space of marine ecosystems under contrasting emission pathways

Timothée Bourgeois[1], Giang T. Tran[2], Aurich Jeltsch-Thömmes[3,4], Jörg Schwinger[1], Friederike Fröb[5], Thomas L. Frölicher[3,4], Thorsten Blenckner[6], Olivier Torres[7], Jean Negrel[1], David P. Keller[2,8], Andreas Oschlies[2], Laurent Bopp[7], Fortunat Joos[3,4]

[1]NORCE Climate & Environment, Bjerknes Centre for Climate Research, Bergen, 5005, Norway
[2]Marine Biogeochemical Modelling, GEOMAR Helmholtz-Zentrum für Ozeanforschung Kiel, Kiel, 24105, Germany
[3]Climate and Environmental Physics, Physics Institute, University of Bern, Bern, 3012, Switzerland
[4]Oeschger Centre for Climate Change Research, University of Bern, Bern, 3012, Switzerland
[5]Geophysical Institute, University of Bergen, Bjerknes Centre for Climate Research, Bergen, 5005, Norway
[6]Stockholm Resilience Centre, Stockholm University, Stockholm, 106 91, Sweden
[7]LMD-IPSL, CNRS, Ecole Normale Supérieure/PSL Res. Univ, Ecole Polytechnique, Sorbonne Université, Paris, 75005, France
[8]Carbon to Sea Initiative, Washington, DC, USA

Correspondence to: Timothée Bourgeois (tbou@norceresearch.no)

Abstract. Anthropogenic greenhouse gas emissions cause multiple changes in the ocean and its ecosystems through climate change and ocean acidification. These changes can occur progressively with rising atmospheric carbon dioxide concentrations, but there is also the possibility of large-scale abrupt, and/or potentially irreversible changes, which would leave limited opportunity for marine ecosystems to adapt. Such changes, either progressive or abrupt, pose a threat to biodiversity, food security, and human societies. However, it remains notoriously difficult to determine exact limits of a "safe operating space" for humanity. Here, we map, for a variety of ocean impact metrics, the crossing of limits, which we define using the available literature and to represent a wide range of deviations from the unperturbed state. We assess the crossing of these limits in three future emission pathways: two climate mitigation scenarios, including an overshoot scenario, and one high-emission no-mitigation scenario. These scenarios are simulated by the latest generation of Earth system models and large perturbed-parameter ensembles with two Earth system models of intermediate complexity. Using this comprehensive model database, we estimate when and at which warming level 4 mitigation limits for 15 different impact metrics are exceeded along with an assessment of uncertainties. We find that under the high-emissions scenario, the two highest limits are exceeded with high probability for marine heatwaves' duration, loss of Arctic summer sea ice extent, expansion of ocean areas that are undersaturated with respect to aragonite, and decrease in plankton biomass. The probability of exceeding a given limit generally decreases clearly under low-emissions scenario. Yet, exceedance of ambitious limits related to steric sea level rise, Arctic summer sea ice extent, Arctic aragonite undersaturation, and plankton biomass are projected to be difficult to avoid (high probability) even under the low-emissions scenario. Compared to the high-emissions scenario, the scenario including a temporary overshoot reduces with high probability the risk of exceeding mitigation limits by year 2100 related to marine heatwave duration, Arctic summer sea ice extent, strength of the Atlantic meridional overturning circulation, aragonite

undersaturation, global deoxygenation, plankton biomass, and metabolic index. Our study highlights the urgent need for ambitious mitigation efforts to drastically minimize extensive impacts and potentially irreversible changes to the world's ocean ecosystems.

1 Introduction

Earth system models (ESMs) are invaluable tools to simulate the climate outcomes of future emission pathways. However, due to computational constraints, ESMs are limited in terms of spatial resolution and complexity of represented processes (Chen et al., 2021). Consequently, it remains notoriously difficult to assess climate change impacts that occur at smaller scales or in systems that are not exhaustively represented in ESMs, especially for essential variables linked to marine biodiversity and marine ecosystems services (Pereira et al., 2013; Balvanera et al., 2022). Large-scale changes in important drivers of marine ecosystem processes (for example, warming, deoxygenation, and acidification) are often taken as a measure of potential ecosystem damage ("ecosystem stressors"). As such changes will usually occur simultaneously, the term "multiple potential ecosystem stressors" has been coined to describe the threat that climate change poses to marine ecosystems (Bopp et al., 2013; Gattuso et al., 2015; Gruber, 2011; Kwiatkowski et al., 2020). To consider the various stressors and management strategies that affect the Earth system, the concept of safe operating space has been proposed (Rockström et al., 2009). For the ocean, a safe operating space refers to the conditions under which marine ecosystems can remain resilient and continue to provide essential services despite ongoing environmental changes and human activities (Nash et al., 2017).

Although it is generally well-known which climate variables will have an adverse impact on ecosystems and societies if they are altered by human activity, exact limits that should not be exceeded are often difficult to define. This might be the case either because impacts occur gradually in synchrony with changes in a driver variable (and it thus remains an ethical or economic question how much damage can be accepted), or because a limit exists but it is highly uncertain. The latter will be the case if tipping points exist in the system, a crossing of which will lead to large and irreversible changes (e.g., Lenton et al., 2008; Armstrong McKay et al., 2022). For ecosystems in particular, the possibility exists that gradual changes in the physical or biogeochemical state may lead to the crossing of tipping points (Heinze et al., 2021). Nevertheless, our knowledge on the impacts of these changes on marine ecosystems is growing. Thermal changes induced by global warming are altering the productivity of some phytoplankton functional types and are reshaping established interspecific competition in marine ecosystems (Kordas et al., 2011; Dutkiewicz et al., 2013; Anderson et al., 2021). The shoaling of the calcium carbonate ($CaCO_3$) saturation horizon due to ocean acidification is threatening calcifying organisms (Orr et al., 2005; Doney et al., 2020). Ocean deoxygenation and the expansion of oxygen minimum zones contribute to marine aerobic habitat loss (Diaz and Rosenberg, 2008; Pinsky et al., 2020; Morée et al., 2023; Fröb et al., 2024). Shifting circulation patterns affect fish migrations and human societies (Van Gennip et al., 2017; Schwinger et al., 2022). Finally, upper-ocean stratification changes alter ocean primary productivity and community structures by exacerbating surface nutrient depletion (e.g., Fu et al., 2016).

In this study, we define a set of 15 impact metrics associated to 4 mitigation limits following the approach of Steinacher et al. (2013). We aim at determining the probability of staying within a given mitigation limit based on scenario simulations from state-of-the-art Earth system models from the latest Coupled Model Intercomparison Project (CMIP6), and two perturbed parameter ensembles from Earth system models of intermediate complexity (EMICs). EMICs are an important modelling tool in climate sciences because of their relatively low computational cost compared to ESMs, which makes them suitable to create large ensembles for uncertainty quantification (e.g., Steinacher et al., 2013; Steinacher and Joos, 2016), and for simulations over long time scales (several 1000 years, e.g., Battaglia and Joos, 2018; Plattner et al., 2008). EMICs have also been extensively used to investigate the Earth system response to strong mitigation scenarios and to carbon dioxide removal (e.g. Jeltsch-Thömmes et al., 2024; Tokarska et al., 2019). Both model types (ESMs and EMICs) have their specific advantages and limitations. The low computational demand of EMICs comes at the cost of resolution and complexity, which remains relatively low. ESMs with their higher resolution and complexity, can usually only be run for a limited number of ensemble members, if any. The CMIP6 ensemble of ESMs is an ensemble of opportunity, and the quantification of uncertainty using this ensemble has, although common practice, certain limitations (e.g., Knutti, 2010). Despite their importance, both model classes (EMICs and ESM) are rarely compared. By applying the same analysis of impact metrics and associated mitigation limits to the same scenarios simulated by both model classes, this study aims to fill this gap.

2 Methods

2.1 Definition of impact metrics and mitigation limits

We use 15 illustrative impact metrics providing a broad spectrum of impacts of climate change on marine ecosystems, and each of them are associated with 4 mitigation limits (Table 1). Mitigation limits are ordered according to the expected severity of impacts when exceeding the limit, that is, exceeding mitigation limit 4 for a given metric is expected to result in more severe impacts than exceeding mitigation limit 1, and correspondingly, staying under limit 1 is more ambitious because a higher emission reduction would be needed to stay below this limit. Mitigation limits at a given level are not necessarily dependent, i.e., they can be exceeded at different time and global warming levels.

A literature review combining observations with simulation studies on critical limits in the ocean system is conducted to define the impact metrics and mitigation limits. While the aim of this study is to define mitigation limits based as much as possible on the literature, many metrics suffer from a lack of knowledge regarding the assessment of actual impacts that an exceedance would have on the Earth system or ecosystem functioning, especially in a multi-stressor context (Williamson and Guinder, 2021). Some physical metrics have been more thoroughly investigated, while biogeochemical metrics are less constrained. Observations and laboratory experiments suggest numerous critical limits for key ecosystem stressors. Moreover, these limits are species-dependent and can vary over a wide range. Thus, for some metrics, we favour limits based on relative changes to characterise reasonably safe levels instead of absolute changes. These choices could be refined through future research and

further dialogue with stakeholders. If the literature does not permit us to define mitigation limits for a specific metric, then we use *ad hoc* limits that cover the simulated mitigation space from very strong mitigation to very little or no mitigation effort.

The impact metrics include six physical parameters, related to surface atmospheric warming, marine heatwaves, steric sea level rise, sea ice extent, and the Atlantic Meridional Overturning Circulation (AMOC), five chemical parameters, related to global and regional ocean acidification and deoxygenation, and four ecosystem parameters, related to productivity, biomass, organic matter export, and metabolic performance.

Physical metrics

Global mean surface air temperature (SAT) is an important metric of the climate system and has strong and direct influences on ecosystems as well as human systems, i.e., many other important indicators and metrics co-vary with temperature. We pick the mitigation limits of 1.5°C and 2°C increase since the 1850-1900 mean based on the Paris agreement (UNFCCC, 2015). Two additional limits of 3°C and 4°C represent temperature limits beyond which severe impacts and the triggering of global tipping elements could be possible (Armstrong McKay et al., 2022; Masson-Delmotte et al., 2021). These limits for global mean SAT increase have also been previously used in Steinacher et al. (2013).

We consider marine heatwaves due to their substantial global and regional impacts on marine ecosystems (Capotondi et al., 2024; Frölicher and Laufkötter, 2018; Smith et al., 2021). We use two definitions of marine heatwaves based on different baselines (Burger et al., 2022; Smith et al., 2025). First, we define a marine heatwave day as the local daily mean sea surface temperature (CMIP6 variable *tos*) exceeding the 90th percentile relative to a fixed seasonally varying 1850-1900 baseline (metric abbreviated MHW_{fix}). In this case, changes in marine heatwaves are driven by both long-term surface ocean warming trends and changes in anthropogenically-forced internal variability. The fixed baseline may be particularly relevant for assessing the risk marine heatwaves pose to organisms with slow adaptation rates. Second, we define a marine heatwave day relative to a shifting-mean baseline (MHW_{shift}), where the 1850-1900 percentile thresholds are adjusted according to the forced mean trend in sea surface temperature (SST). The forced trend is identified using a smoothing "Enting" spline (Enting, 1987) with a 80-yr cut off period. In the shifting-mean approach, changes in marine heatwave duration are primarily driven by changes in anthropogenically-forced internal variability, while the long-term warming trends is already accounted for in the baseline (Burger et al., 2022; Deser et al., 2024). The choice between a fixed or shifting baseline depends on the specific application. For example, the shifting-mean case may better capture the risks posed to organisms that can adapt to long-term warming trends. For both definitions, we (1) calculate the global annual mean duration of marine heatwaves, and (2) deduce the anomaly relative to the 1850-1900 period to normalize model-dependent internal variability. Given the lack of strong observational constraints on a global marine heatwave exceedance metric, we distribute uniformly the mitigation limit values of MHW_{fix} over the year as 90, 180, 270, 360 days (the latter representing an almost permanent heatwave) while we distribute the limits of MHW_{shift} over the range of projected values under the scenarios used in this study with 4, 6, 8, and 10 days.

The third physical metric chosen is the rise of steric sea level (SSL). Sea level is rising at accelerating rates, which poses a significant challenge to coastal ecosystems and community livelihoods. We are only considering the SSL rise because the

models used in our study do not simulate the melting of glaciers and ice sheets. While strongly connected to global warming, SSL rise shows a delayed response due to the long thermal lag of the ocean system (Levermann et al., 2013). The SSL rise is estimated to account for 40 % of the total sea-level rise of 0.2 m today, i.e., the current estimated SSL rise is estimated at around 0.08 m (Church et al., 2011; Fox-Kemper et al., 2021; WCRP Global Sea Level Budget Group, 2018). O'Neill et al. (2017) estimate that risks related to SSL rise are at a moderate level at about 0.1 m above the 1986-2005 level, and transition to high risks are expected at around 1 m above the same reference level. Hinkel et al. (2014) find that under no adaptation, 0.25-1.23 m of global sea-level rise (i.e., 0.1 to 0.5 m of SSL rise assuming a constant steric to sea level rise ratio) in 2100 would expose 0.2 - 4.6 % of the global population to flooding annually. Hermans et al. (2021) found a mean SSL rise of 0.27 m in 2100 simulated by CMIP5 and CMIP6 ensembles under high-emissions scenarios. According to Hague et al. (2023), the current sea level rise is already expected to increase flood frequencies at a level of 0.2 m of sea level rise (or 0.08 m of SSL rise). Thus, we chose to define the four limits as 0.1, 0.2, 0.3, and 0.4 m of SSL rise relative to the period 1850-1900, to encompass the range found in the above-mentioned literature.

Changes in summer Arctic sea-ice extent have a direct impact on the climate system through the albedo feedback. Furthermore, a substantial reduction of Arctic sea ice could threaten the livelihood of organisms that depend upon habitats provided by sea ice. Arctic sea ice is projected to decline, and an ice-free summer state is expected even with a stabilised global warming of 1.5°C (~1 % chance of individual ice-free years by the end of the century; Pörtner et al., 2019). Here, the summer ice-free state is defined as a September sea ice extent below 10^6 km^2. We further define three more limits up to 4 x 10^6 km^2 following the projected range from Stroeve et al. (2012) and Peng et al. (2020). Exceedances of the 4 x 10^6 km^2 limit has already been observed in 2012 and 2020 (https://nsidc.org/, visited on May 21st, 2025).

A collapse of the Atlantic meridional overturning circulation (AMOC) is often considered a more distant tipping point (Lenton, 2012) even though recent literature estimated that we cannot rule out that AMOC is on course to collapse (Van Westen et al., 2024). The estimated probabilities from expert elicitation for a shutdown of AMOC (until 2100) is 0-0.2 for low (<2°C), 0-0.6 for medium (2-4°C), and 0.05-0.95 for high climate change (4-8°C), according to Zickfeld et al. (2007) and Kriegler et al. (2009). A weakening of the AMOC this century is expected (Pörtner et al., 2019; Fox-Kemper et al., 2021), which can cause, for example, changes in the rainfall, storm frequency in Northern Europe and a decrease in marine productivity in the North Atlantic (Pörtner et al., 2019). We compute the strength of the AMOC as the vertical maximum of the stream function at 26°N following Weijer et al. (2020). As for the limits, despite a growing body of literature on the historical and projected evolution of the AMOC, we still lack sufficiently long observation-based time series, knowledge, and scientific consensus to understand if the AMOC is already experiencing a decline exceeding natural variability, and if such a decline is attributed to anthropogenic forcing (Jackson et al., 2022; Latif et al., 2022; Lobelle et al., 2020; Terhaar et al., 2025). Due to the absence of more robust knowledge, we choose four limits at 20, 25, 30, and 40% decline relative to 1850-1900 to cover the range of model responses (Weaver et al., 2012; Weijer et al., 2020).

Ocean acidification metrics

Ocean omega aragonite (Ω_{arag}), or the level of saturation of the least-stable form of calcium carbonate in seawater, is a common indicator of the potential for biotic calcification (Gazeau et al., 2007). Ocean acidification could lead to undersaturation ($\Omega_{arag}<1$) and dissolution of calcium carbonate in parts of the surface ocean during the 21st century, which can have detrimental effects on marine ecosystems (Orr et al., 2005). Studies have shown that no prominent present-day coral reefs exist in environments with $\Omega_{arag}<3$ (Guinotte et al., 2003; Hoegh-Guldberg et al., 2007; Kleypas et al., 1999a). A lower limit of $\Omega_{arag}<1.5$ has been used previously to indicate water masses which may be stressful to larvae of shellfish such as oysters (Ekstrom et al., 2015; Gimenez et al., 2018). For $\Omega_{arag}<1.5$, calcifying organisms have trouble forming shells during the first few days of their life (Waldbusser et al., 2015). Guinotte et al. (2006) estimated that over 95 % of cold water biotherm-forming corals were found in water masses that were supersaturated ($\Omega_{arag}>1$). We define three ocean acidification metrics in terms of area fractions. The first two metrics, abbreviated A_{SO} and A_{Arctic}, are respectively the surface area fractions of the Southern Ocean (Nouth of 50°S) and the Arctic Ocean (North of 70°N) undersaturated with respect to aragonite ($\Omega_{arag}<1$; annual mean), which means that seawater becomes corrosive to aragonitic shells (Doney et al., 2009; Fabry et al., 2009). The selected limits for these metric range from 20 % to 80 % following Steinacher et al. (2009, 2013). The third ocean acidification metric, $A_{\Omega>3}$, addresses areas with high saturation states ($\Omega_{arag}>3$) that are mainly found in the tropics and subtropics (Kleypas et al., 1999b). We define this variable as the percentage of the global ocean surface area with $\Omega_{arag}>3$ that has been lost since pre-industrial times and select limits from 50 % to 100 % (Steinacher et al., 2013). For the sake of readability, these metrics are sometimes referred in the text to Southern Ocean $\Omega_a<1$, Arctic Ocean $\Omega_a<1$ and Global Ocean $\Omega_a>3$, respectively.

Other biogeochemical metrics

Marine species have been observed to die after exposure to a wide range of critical oxygen (O_2) levels, from 8.6 mg O_2 L^{-1} (ca. 275 µmol L^{-1}) to anoxia (Vaquer-Sunyer and Duarte, 2008). Critical O_2 levels are largely species- and stage-specific (Ekau et al., 2010), making it challenging to define common limits. Globally, dissolved O_2 is projected to decline by 1.81 to 3.45 % by the year 2100 under CMIP5 representative concentration pathways (RCP) (Bopp et al., 2013). Subsurface (100-600 m) O_2 is projected to decline by 3.1-4 % under RCP8.5 and 0.1-0.5 % under RCP2.6. The projected decline in the subsurface dissolved O_2 concentration for CMIP6 models under their shared socioeconomic pathways (SSP) vary from -6.36 to -13.27 µmol L^{-1} by the end of the century (Kwiatkowski et al., 2020). The equivalent range for CMIP5 models under RCP scenarios is from -3.71 to -9.51 µmol L^{-1}. Due to large differences between models and when compared to observations, we decided to define relative limits for two metrics: mean global full-depth O_2 concentration and volume of hypoxic waters above 1000 m depth (i.e., waters with <63 µmol L^{-1}; Limburg et al., 2020).

The decline of marine net primary productivity (NPP) is considered one of the primary stressors of open ocean ecosystems (Bopp et al., 2013). Mitigation limits for marine NPP are defined in terms of relative changes for the same reason as above. Kwiatkowski et al. (2020) shows changes from -0.56 ± 4.12 % under SSP1-2.6 to -2.99 % ± 9.11 % under SSP5-8.5 for CMIP6 models, while the range for CMIP5 models is from -3.42 ± 2.47 % under RCP2.6 to -8.54 ± 5.88 % under RCP8.5 until year 2100. Thus, we set the limits to 2, 3.5, 4 and 8 % relative to 1850-1900. In addition to NPP, we consider changes in plankton

biomass (ΔBiomass) because projected plankton biomass has been considered as a more robust metric reflecting the impact of climate change on marine ecosystems (Bopp et al., 2022; Tittensor et al., 2021). The ΔBiomass metric represents the change in the sum of phytoplankton and zooplankton biomass (CMIP6 variables *zooc* and *phyc*) and its limits are the same as those for NPP. We excluded the model CNRM-ESM2-1 for this metric due to a large inconsistent variability found over the historical period, which has been attributed to mesozooplankton biomass.

We consider changes in the upper ocean metabolic index and changes in particulate organic matter (POM) export between 30°S and 30°N as indicators of the compound effects of warming and oxygen changes on viable habitat and the survival of marine species (Battaglia and Joos, 2018). The metabolic index, Φ, is defined as the ratio of O_2 supply to an organism's resting O_2 demand. Warming ocean and lower partial pressure of O_2 is expected to reduce the globally averaged upper ocean (0 – 200 m) metabolic index, which was shown to restrict viable habitats (Deutsch et al., 2015). Φ has been calculated following Fröb et al. (2024) using the median ecophysiotype of the 61 species described in Deutsch et al. (2020), without considering biomass distribution. The export of POM is the primary food source for deep-sea organisms. Thus, the POM export between 30°S and 30°N serves as an indicator of food availability in deep sea habitats. The limits of 4, 6, 8, and 10 % for these two indicators are based on the result of Battaglia and Joos (2018).

Table 1. Impact metrics and corresponding mitigation limits for changes until year 2100. Mitigation limits that are considered for ESMs only are marked with an asterisk.

Impact metric	Description	Level 1	Level 2	Level 3	Level 4	Unit
ΔSAT	Increase in mean annual global surface atmospheric temperature relative to 1850-1900	1.5	2	3	4	°C
MHW_{fix}*	Global mean duration of marine heatwaves within a year, relative to a fixed baseline	90	180	270	360	day
MHW_{shift}*	Same as MHW_{fix} (line above), but using a shifting baseline approach	4	6	8	10	day
ΔSSL	Mean annual steric sea level rise relative to 1850-1900	0.1	0.2	0.3	0.4	m
SIE*	Arctic September sea-ice extent	4	3	2	1	10^6 km^2
ΔAMOC	Change in mean annual strength of the AMOC relative to 1850-1900	-20	-25	-30	-40	%
A_{SO}	Mean annual area proportion of Southern Ocean surface waters (south of 50°S) with aragonite undersaturation ($\Omega_{arag}<1$)	20	40	60	80	%

A_{Arctic}	Mean annual area proportion of Arctic Ocean surface waters (north of 70°N) with aragonite undersaturation ($\Omega_{arag}<1$)	20	40	60	80	%
$A_{\Omega<3}$	Mean annual area proportion of global ocean surface waters with $\Omega_{arag}<3$	50	70	90	100	%
Hypoxic ΔO_2	Change in mean annual volume of hypoxic waters (<63 umol L^{-1}) above 1000 m relative to 1850-1900	2	4	6	8	%
Global ΔO_2	Change in mean annual global O_2 content relative to 1850-1900	-1.8	-2.4	-2.6	-3.5	%
ΔNPP*	Change in mean annual depth-integrated net primary production relative to 1850-1900	-2	-3.5	-4	-8	%
ΔBiomass*	Change in mean annual depth-integrated plankton biomass relative to 1850-1900	-2	-3.5	-4	-8	%
ΔΦ	Change in mean annual upper-ocean (depth < 400 m) metabolic index relative to 1850-1900	-5	-10	-15	-20	%
ΔPOM	Change in mean annual particulate organic matter flux at 100 m depth (30°N-20°S) relative to 1850-1900	-4	-6	-8	-10	%

2.2 CMIP6 Earth system model ensemble

Our CMIP6 model ensemble is composed of 9 ESMs (Table 2). This ensemble is based on the one used in Canadell et al. (2021), but excluding model family duplicates, and using the variant r1i1p1f1 (or equivalent). All ESMs use ocean components with a nominal horizontal resolution of about 1° with grid refinements of up to about 1/3° both poleward and at the equator. We use 3 scenarios from CMIP6 covering the period 2015-2100, which are initialized from the end of the historical simulation (1850 to 2014) that is based on estimates of historical forcings (O'Neill et al., 2016). These scenarios cover very different possible futures: The low-emission, high-mitigation scenario SSP1-2.6 assumes that the world gradually shifts toward a more sustainable pathway, and that early and consistent climate mitigation limits the end-of-century radiative forcing to 2.6 W m^{-2}. In contrast, the SSP5-8.5 scenario assumes resource-intensive, strong economic growth based on the exploitation of fossil fuel reserves and no climate mitigation. The very high carbon dioxide (CO_2) emissions in this scenario lead to a radiative forcing of 8.5 W m^{-2} at the end of this century. The SSP5-3.4-OS scenario follows the SSP5-8.5 pathway up to year 2040. Then, strong

climate mitigation policies are implemented, including carbon dioxide removal from the atmosphere, leading to a peak and decline in surface temperature and a final radiative forcing level of 3.4 W m^{-2} in 2100. To use the same model ensemble for all scenarios, we excluded models that do not provide SSP5-3.4-OS.

Table 2. CMIP6 ensemble and variable availability per model.

Model	Reference	Variable availability
ACCESS-ESM1-5	Ziehn et al. (2020)	SAT, SIE, O_2, Φ, MHW, AMOC, Ω_{arag}, SSL, POM, NPP
CanESM5	Swart et al. (2019)	SAT, SIE, O_2, Φ, MHW, Biomass, AMOC, Ω_{arag}, SSL, POM
CESM2-WACCM	Danabasoglu et al. (2020)	SAT, SIE, Biomass, AMOC, Ω_{arag}, POM, NPP
CMCC-ESM2	Cherchi et al. (2019)	SAT, O_2, Φ, MHW, Biomass, Ω_{arag}, SSL, POM, NPP
CNRM-ESM2-1	Séférian et al. (2019)	SAT, SIE, O_2, Φ, MHW, AMOC, Ω_{arag}, SSL, POM, NPP
IPSL-CM6A-LR	Boucher et al. (2020)	SAT, SIE, O_2, Φ, Biomass, AMOC, Ω_{arag}, SSL, POM, NPP
MIROC-ES2L	Hajima et al. (2020)	SAT, SIE, O_2, Φ, Biomass, AMOC, Ω_{arag}, POM, NPP
NorESM2-LM	Seland et al. (2020)	SAT, SIE, O_2, Φ, MHW, Biomass, AMOC, Ω_{arag}, SSL, POM, NPP
UKESM1-0-LL	Sellar et al. (2019)	SAT, SIE, O_2, Φ, MHW, Biomass, Ω_{arag}, SSL, POM, NPP

All ESM model outputs used in this study have been regridded to a 1°-resolution regular grid (360x180 grid cells) before analysis. Since most of the impact metrics are expressed as a change relative to the period 1850-1900, model biases would only be an issue for the analysis presented here if the response to forcing would significantly depend on the baseline state. However, we removed potential model drifts from two sensitive metrics (ΔSSL and Global ΔO_2) by calculating the difference between the projected signal and its equivalent from the corresponding preindustrial experiment (piControl). To account for carbonate chemistry biases in the present-day mean state simulated by the CMIP6 ESMs, we follow the methodology of Terhaar et al. (2020). Changes in aragonite saturation state (Ω_{arag}) have been computed offline using mocsy 2.0 (Orr and Epitalon, 2015) from regridded annual CMIP6 model outputs of dissolved inorganic carbon (DIC), alkalinity, sea water temperature (T), and sea water salinity (S). These modelled changes have then been added to the contemporary saturation state that we derived from the observation-based GLODAPv2 data product for DIC and alkalinity (Lauvset et al., 2016), and the World Ocean Atlas 2013 for T and S (Locarnini et al., 2013; Zweng et al., 2013).

For all impact metrics, time series have been smoothed using a 20-year running mean before identifying the years and global warming levels when a certain mitigation limit is exceeded. The exceedance is identified by the time and global warming level at which a given mitigation limit is exceeded for the first time. This definition does not account for "overshooting" limits of an impact metric. Cases where a limit is first exceeded, but the system returns to a state below the limit later in time, is counted

as an exceedance. Nevertheless, we provide analysis that allows for identifying cases where such overshooting of limit happens (Figs. 3 and 4).

Some mitigation limits might be exceeded by only a part of all available models or ensemble members, while other mitigation limits might be exceeded by all models or ensemble members within the time horizon of the scenario simulations (until 2100). If a model does not exceed a given mitigation limit, we interpret this as an exceedance in the last year of the simulation (year 2100). This approach is conservative in the sense that it assigns the earliest possible exceedance year (the unknown true exceedance year of this model is later, or the model might not exceed the limit at all), and it ensures that all information provided by the model ensemble is used. A similar approach is applied along the global warming dimension, by attributing the highest warming level reached by the model under the given scenario to models not exceeding a given mitigation limit. Consequently, our exceedance estimates are characterised in terms of uncertainty and probability. We define exceedance uncertainty as the interquartile range of an exceedance estimate in a given model ensemble for a given experiment, impact metric, and limit. We define exceedance probability as the proportion of models exceeding a mitigation limit across all models that provide data for a given impact metric and limit (i.e., here we exclude models that did not exceed the limit within the simulation period). We assign high probability to an estimate of exceedance time (or warming level) if a mitigation limit is exceeded by at least 80 % of our CMIP6 ensemble (i.e., at least 8 out of 9 ESMs) or of the ensemble members of an individual EMIC, medium probability if 50-79 % of the models or ensemble members exceed the limit, and low probability if less than 50 % of models or ensemble members exceed the limit. This approach avoids the use of ensemble means, and uncertainty intervals such as ensemble standard deviation to define exceedances, from which a lot of information on the distribution of exceedances within the ensemble is lost leading to an underestimation of the resulting exceedance uncertainty. We will further discuss this issue below with some examples. We note that there are small differences as to which CMIP6 ESMs can be used for which metric, since not all models provide all data necessary for all impact metrics (Table 2).

2.3 Large perturbed-parameter ensembles from two Earth System Models of Intermediate Complexity

In addition to output from CMIP6 ESMs, we also analyse scenario simulations of two Earth system models of intermediate complexity (EMICs), the Bern3D-LPX model and the University of Victoria Earth System Climate Model (UVic). Both EMICs have simulated large perturbed-parameter ensembles (PPE) to estimate the range of parametric (model) uncertainty. The EMIC PPEs were run over the historical period as well as for the SSP1-2.6, SSP5-3.4-OS, and SSP5-8.5 scenarios. Ensemble generation, sampled parameters, and calculation of ensemble member skill scores based on observations differ between the two models and are briefly outlined below.

Bern3D-LPX model

The model setup, ensemble generation, and evaluation as well as the experimental protocol of the Bern3D-LPX ensemble are the same as detailed in Jeltsch-Thömmes et al. (2024). The model features a three-dimensional dynamic ocean (Edwards et al., 1998; Müller et al., 2006) including sea-ice, a single-layer energy and moisture balance model of the atmosphere (Ritz et al.,

2011), and a comprehensive terrestrial biosphere component (LPX-Bern v1.5) with dynamic vegetation, fire, nitrogen, nitrous oxide, methane, permafrost, peatland, and land-use modules (Lienert and Joos, 2018).

The sampling approach for the PPE builds upon work by Steinacher et al. (2013) and has been used thereafter in several follow-up studies (e.g., Steinacher and Joos, 2016; Battaglia et al., 2016; Battaglia and Joos, 2018; Lienert and Joos, 2018). A 1000-member PPE is generated from the prior distributions of 27 key model parameters using Latin hypercube sampling (Mckay et al., 2000; Steinacher et al., 2013).

To reduce uncertainties, we exploit a broad set of observation-based data (Fig. A1) to constrain the model ensemble to realisations that are compatible with observations, thereby probing both the mean state and the transient response in space and time of the ensemble members. Further details on the methods used to constrain the Bern3D-LPX model ensemble with observations are provided in Jeltsch-Thömmes et al. (2024).

UVic ESCM v2.10

The UVic ESCM v2.10 (Mengis et al., 2020; Weaver et al., 2001) has a three dimensional ocean with a horizontal resolution of 3.6° longitude, 1.8° latitude, and 19 vertical levels. The atmosphere is represented by a two-dimensional energy-moisture balance model with the same horizontal resolution (Fanning and Weaver, 1996). The oceanic physics follows the Modular Ocean Model version 2 (MOM2) (Pacanowski, 1996) and the ocean biogeochemistry model is outlined by (Keller et al., 2012). A thermodynamic-dynamic sea ice model (Bitz et al., 2001) employing elastic visco-plastic rheology (Hunke and Dukowicz, 1997) is coupled to the ocean. The terrestrial component accounts for vegetation dynamics and incorporates five different plant functional types (Meissner et al., 2003). Additionally, the model includes a representation of permafrost carbon (MacDougall et al., 2017) using a diffusion-based scheme, which approximates the process of cryoturbation.

We adopt a similar approach as described in Jeltsch-Thömmes et al. (2024) for the Bern3D-LPX model to generate the PPE and compute PPE member's scores based on observations. An emulated ensemble of 1978 members was weighted using this score and used for all statistical computations in this work (see appendix A for details).

3 Results and Discussion

3.1 CMIP6 ESM

The uncertainty, and probability related to the time and global warming levels at which mitigation limits are exceeded are highly variable across impact metrics, limits, and scenarios (Figs. 1 and 2). The probability in exceedance estimates generally decreases with higher mitigation limits, since generally less models exceed the higher mitigation limits. Note that the interquartile ranges in Fig. 1 are extended toward or up to 2100 in case that only some of the ESMs exceed a given limit, because of our choice to assign the year 2100 as time of exceedance for those models. All the reported median exceedances related to the most ambitious mitigation limit (limit 1) are projected to occur in the short and mid term (before 2060) for all scenarios. If mitigation limit 1 is exceeded with high probability (marked by full size black dots in Figs. 1 and 2) in all scenarios, the median time of exceedance is generally very similar across scenarios (ΔSAT, ΔSSL, SIE, Arctic Ocean Ω_a<1, ΔBiomass

315), because during earlier times the three scenarios share the same historical forcing or have only slightly diverged. Also, before 2040, the two scenarios of the SSP5 family are identical by construction, such that if all models exceed a mitigation limit before 2040, the median exceedance time is identical for SSP5-3.4-OS and SSP5-8.5. Metrics related to surface ocean aragonite saturation state (Arctic Ocean Ω_a<1, Southern Ocean Ω_a<1 and Global Ocean Ω_a<3) show particularly narrow uncertainties over the time dimension, but not over the global warming levels. This is consistent with the findings of Terhaar et al. (2023) 320 showing that projections with prescribed atmospheric CO_2 yield an unrealistic small uncertainty for surface ocean acidification, because the forcing agent (atmospheric CO_2) is the same across all ensemble members. If projections target a certain temperature level, a more relevant estimate of uncertainty can be obtained because variations of climate sensitivity across ensemble members translate into different levels of atmospheric CO_2 at the targeted temperature, and hence into different levels of surface ocean acidification. Lower exceedance probability and larger difference in the timing of exceedance are found 325 for ΔPOM, ΔNPP, global ΔO2, and hypoxic ΔO2. The lower probability in exceedance of ΔNPP mitigation limits across all scenarios is consistent with the high uncertainty in ΔNPP projections found by Kwiatkowski et al. (2020). In contrast, the higher exceedance probability linked to the metric ΔBiomass is consistent with the findings of Tittensor et al. (2021), emphasising that Biomass is a more robust metric for assessing impacts of climate change on marine ecosystems than NPP. Substantial uncertainties in global ΔO_2 were found in earlier multi-model studies (Cocco et al., 2013; Hameau et al., 2020) , 330 which are reflected by the lower probability of exceedance estimates. These uncertainties can be explained by the uncertain balance between O_2 supply from physical mixing and advection, and O_2 consumption from remineralization of organic matter. Uncertainties remain also on how these processes would respond to rising CO_2. Regarding subsurface O_2 projections, Frölicher et al. (2016) identified model structure and parametrization as the second source of projection uncertainty, consistent with the results presented in Figs 1 and 2.

335 The 20-year moving averaging applied to the time series mostly removes interannual to decadal variability and emphasises the signal induced by the different radiative forcing. However, metrics with large internal variability, like the AMOC strength, can still show exceedance distribution not entirely consistent with the different radiative forcing levels applied in the emissions scenarios (Figure 1, limit 2). Similarly, composite metrics such as ΔBiomass (i.e. sum of phytoplankton and zooplankton biomass) include interactive dynamic responses that lead to inconsistent responses with respect to the different radiative forcing 340 levels for some models with exceedances only 2 to 3 years earlier in SSP1-2.6 compared to SSP5-8.5. Hence, differences between scenarios in exceedance timing of around 10 years should not be considered significantly different (i.e., they can be considered as occurring simultaneously).

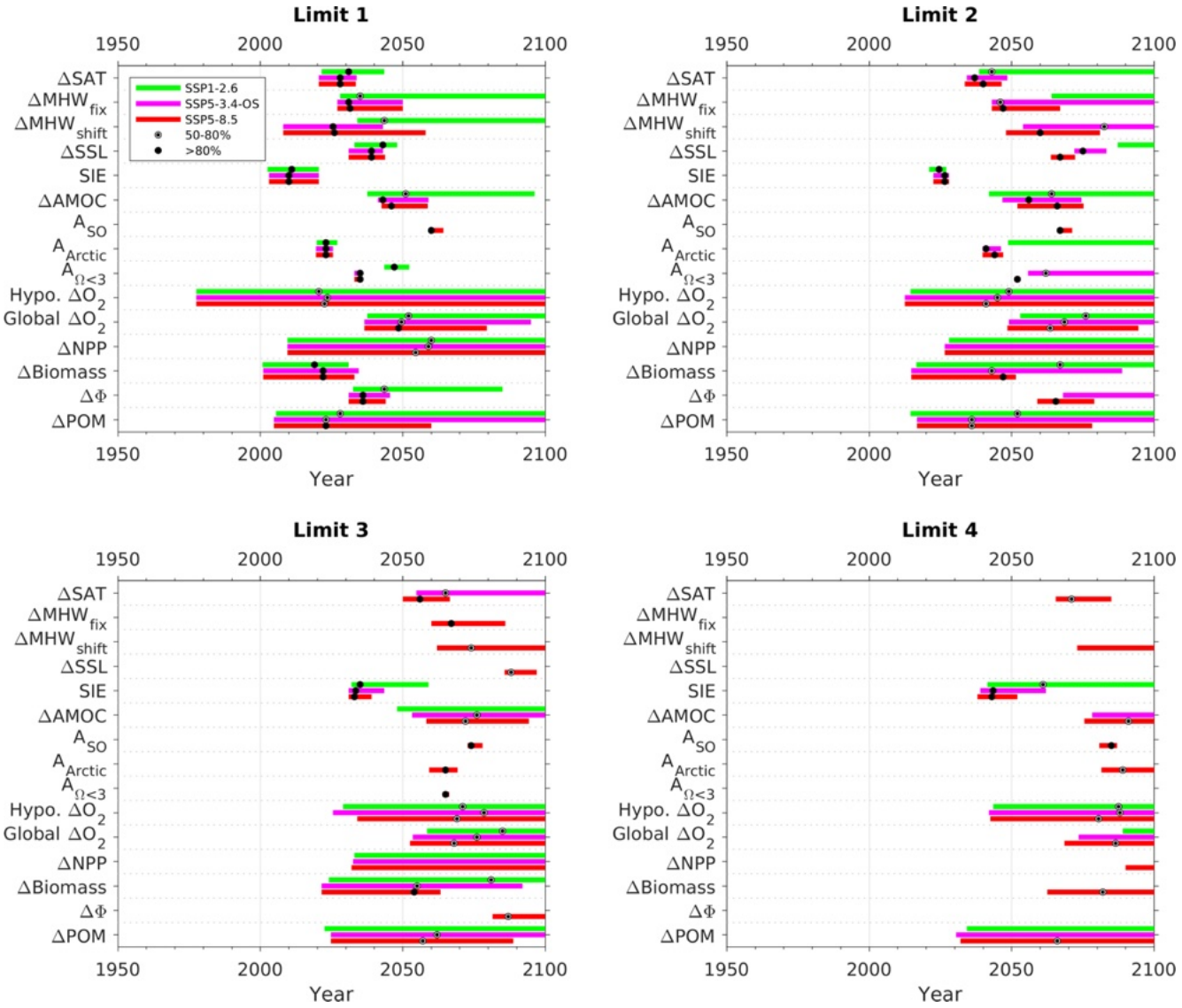

Figure 1: Box plots showing the distribution of exceedance years for each mitigation limits of the impact metrics (abbreviations follow Table 1) for CMIP6 models. Green, purple and red colors depict the three scenarios, i.e., historical-SSP1-2.6, historical–SSP5-3.4-OS and historical–SSP5-8.5. Boxes' lengths and circled black dots depict the interquartile range and the ensemble median, respectively. The size of the black dots indicates the exceedance probability defined as the proportion of models exceeding a mitigation limit across the models providing data for a given impact metric (Full size: >80 %, half size: 50-80 %). The median of low probability exceedances (<50% of models) are not shown.

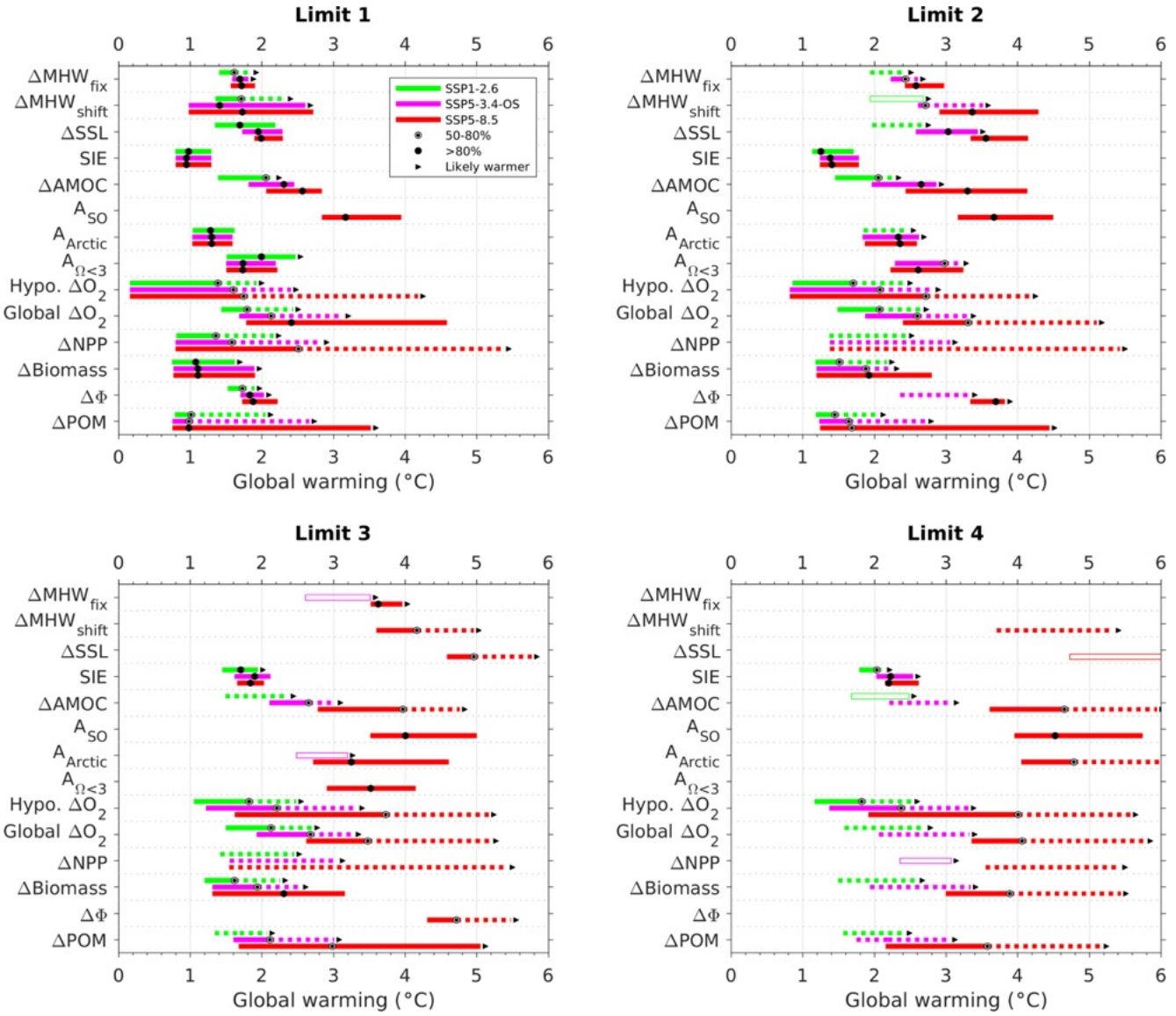

Figure 2: Same as Figure 1, but relative to global warming in degree Celsius during this century instead of time. Cases with very low probability (<25%) are displayed as empty rectangles, using the interquartile range as in Figure 1. Median symbols are not shown for these cases. Low probability cases in the 25–50% probability range are represented by dashed bars covering the interquartile range, without median symbols either. Black arrows pointing toward warmer levels emphasize that the limit would likely be exceeded only at warmer global warming levels. Such arrows are added to all cases in the 50—100% probability range (100% excluded). Medium probability cases with 50–80% have interquartile ranges shown as plain bars with median symbols, and dashed bars over the 50th– 75th percentile range to highlight the uncertainty of the 50th–75th percentile range. Finally, cases with probability >80% follow Figure 1's legend (plain bars over interquartile range with median symbol).

For the less ambitious mitigation limits, exceedance time estimates generally move towards later times and higher warming levels, and the exceedance probability decreases (less models exceed the less ambitious mitigation limits). In the low emission scenario SSP1-2.6, limit 4 is exceeded by less than 20 % of the CMIP6 ESMs for any of the impact metrics due to the stringent

climate mitigation implemented in this scenario. Exceedances occur generally at lower global warming level under scenarios with lower radiative forcing (Fig. 2). For high probability cases, this is due to the inherent inertia from some metrics (e.g., Fig. 2, limit 1, ΔSSL) that eventually leads to an exceedance even under the global warming stabilization induced by SSP1-2.6 scenario. For low probability cases, this observation is only the result of the default attribution of the highest warming level reached to models not exceeding a given limit (Fig. 2, limit 4, ΔBiomass).

If we focus on exceedance estimates that have a high probability (i.e., where more than 80 % of models exceed the mitigation limit), we can provide an estimate of the time when mitigation limits are likely to be exceeded (Figs. 3 to 6). The first mitigation limit of Arctic Ocean Ω_a<1 (20% of undersatured surface waters) is likely already passed in the CMIP6 model ensemble in all scenarios, consistent with the findings of Terhaar et al. (2021). The first mitigation limit of SIE (4 10^6 km^2) is expected to be passed during 2013-2034 (median year 2023). So far, according to satellite-based estimates, Arctic summer sea-ice extent fell below 4 10^6 km^2 in 2012 and 2020 (https://nsidc.org/, visited on May 21st, 2025). The fourth level of mitigation limits is exceeded with high probability only for SIE in SSP5-3.4-OS and SSP5-8.5, as well as for Southern Ocean Ω_a<1 in SSP5-8.5.

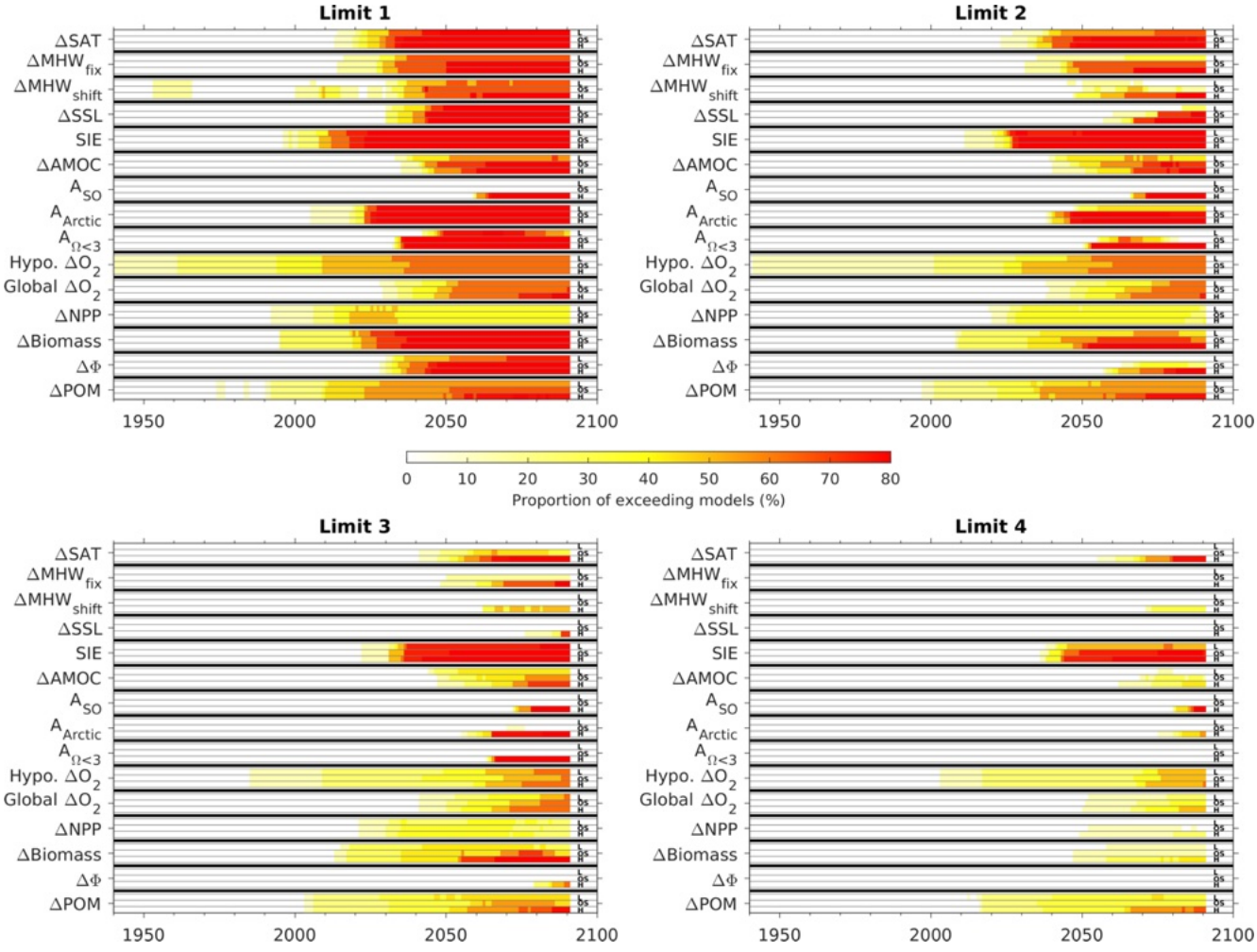

Figure 3: Proportion of models exceeding a given mitigation limit of the impact metrics compared to the available models for each metric. Abbreviations are included for SSP1-2.6 (L), SSP5-3.4-OS (OS) and SSP5-8.5 (H).

Avoiding emissions as high as in the SSP5-8.5 scenario and following an emission pathway similar to SSP5-3.4-OS will likely avoid an exceedance of any of the mitigation limits for ΔMHW_{shift}, Southern Ocean $\Omega_a<1$, Global ΔO_2 , and ΔPOM during this century. In addition, avoiding the SSP5-3.4-OS scenario by early mitigation (as in SSP1-2.6) will likely avoid exceedances of any mitigation limit related to ΔMHW_{fix}, $\Delta AMOC$, $\Delta Biomass$, and $\Delta\Phi$ until year 2100. The mitigation limits of ΔSAT, ΔSSL, SIE, Arctic Ocean $\Omega_a<1$, $A_{\Omega<3}$, and $\Delta Biomass$ are likely to be exceeded across all scenarios. The effect of ambitious mitigation in SSP5-3.4-OS after 2040 can be seen for ΔSAT, ΔSSL, SIE, and $\Delta AMOC$. For these metrics, some of the mitigation limits are first exceeded around mid-century, but later this exceedance is reversed. The uncertainty of hypoxic ΔO_2, global ΔO_2, ΔNPP, and ΔPOM projections does not allow us to conclude with confidence that none of the corresponding mitigation limits will be exceeded due to their attributed low probability (Fig. 4).

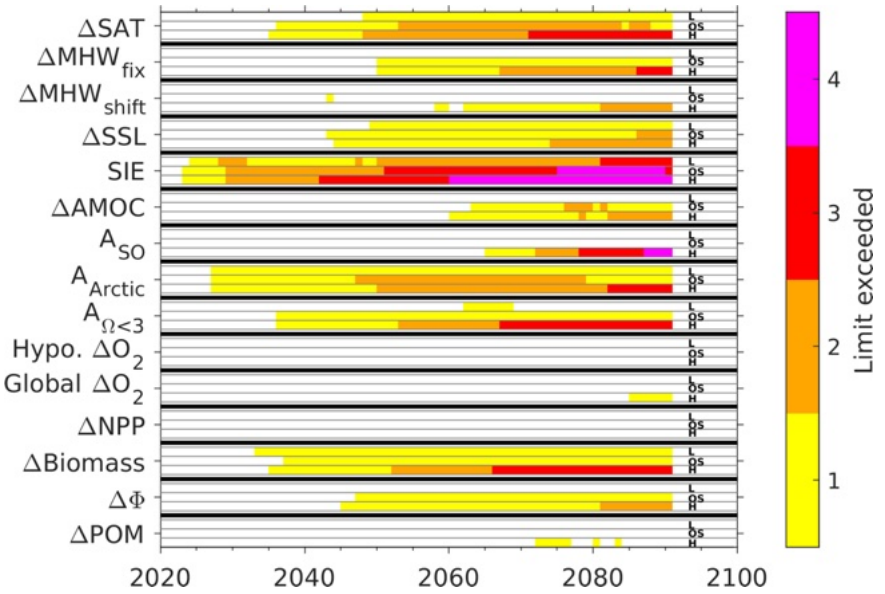

Figure 4: Time periods where mitigation limits are exceeded with high probability according to the CMIP6 model ensemble (>80 % of models) for each impact metrics and for the scenarios SSP1-2.6 (L), SSP5-3.4-OS (OS) and SSP5-8.5 (H).

In Figs. 5 and 6, the summary of high probability exceedance estimates for all impact metrics is quite conservative, since (1) high probability is defined as at least 80 % of models exceeding a limit (i.e., at least 8 out 9 models, which is practically 88 %) and (2) medium probability exceedances (where up to 79 % of the CMIP6 models would show an exceedance of a given mitigation limit) are not included. For the low-emission scenario, already the most ambitious level of limits of 5 impact metrics (ΔSAT, ΔSSL, SIE, Arctic Ocean Ω_a<1, and ΔBiomass) is exceeded with high probability, two of them as early as in the near-term period (2021-2040). In contrast, even the third and fourth set of limits are exceeded with high probability in the high-emission SSP5-8.5 scenario, particularly toward 2100. The absence of high probability in the exceedance for hypoxic ΔO_2, global ΔO_2, ΔNPP, and ΔPOM is explained partly by a model disagreement within our CMIP6 ensemble. Another reason for low-to-medium probability in the exceedance for global and hypoxic ΔO_2 and ΔSSL before year 2100 is that changes in subsurface and whole ocean parameters have been shown to accrue beyond year 2100 and aggravate over many centuries due to the long overturning time scales of the ocean (Battaglia and Joos, 2018). There is a very clear effect of the ambitious mitigation assumed in SSP5-3.4-OS after 2040 in all timeseries of impact metrics, such that the significantly lower exceedance rate of mitigation limits, particularly by the end of the century, clearly illustrated the benefits of stringent and ambitious mitigation. Some metrics show strong hysteresis in response to cumulative carbon emissions (Boucher et al., 2012; Jeltsch-Thömmes et al., 2020; Samanta et al., 2010; Santana-Falcón et al., 2023). Due to that hysteresis behavior, sustained negative emissions are required to return to and stay under a specific limit, particularly for high climate sensitivities and peak-and-decline scenarios with carbon dioxide removal (Jeltsch-Thömmes et al., 2020). This aspect needs to be emphasized in the case

of our study due to the use of simulations ending in 2100, implying that some metrics could return below more ambitious limits beyond 2100 under strong mitigation scenarios.

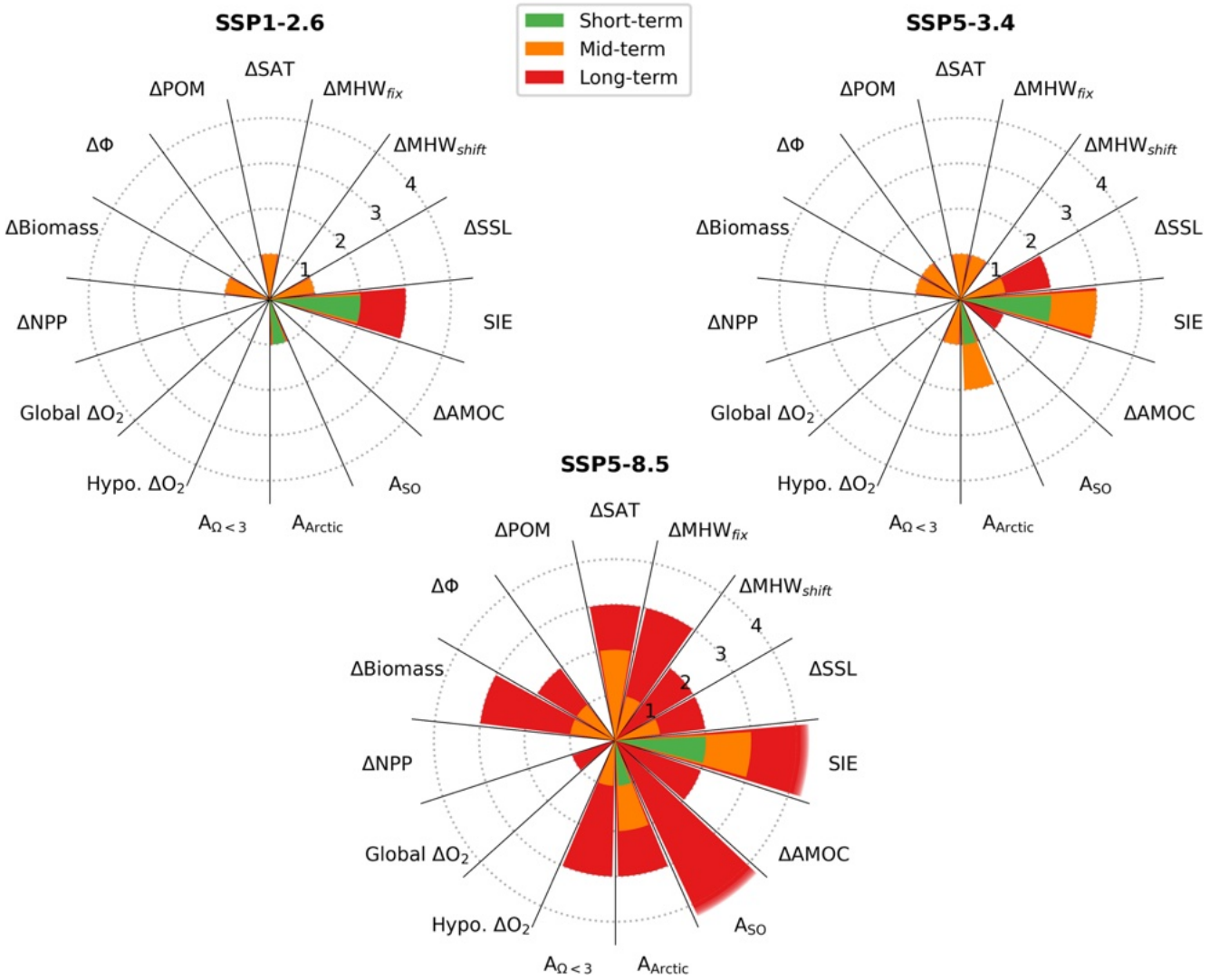

Figure 5: Exceedance of mitigation limits with high probability (>80 % of the CMIP6 models) in the near-term (2021-2040), mid-term (2041-2060) and long-term (2081-2100) periods under (left) SSP1-2.6, (right) SSP5-3.4-OS and (middle) SSP5-8.5 scenarios.

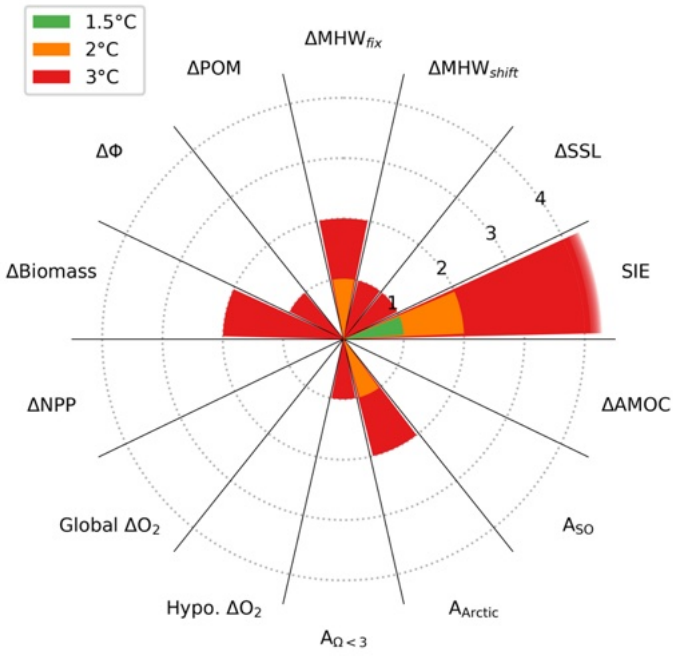

Figure 6: Same as Figure 5, but according to global warming levels (1.5°C, 2°C and 3°C) under the SSP5-8.5 scenario. Therefore, ΔSAT is not shown.

3.2 EMIC & ESM comparison

There is broad agreement for a range of variables on the exceedances of limits between the CMIP6 and the two skill-weighted EMIC ensembles under SSP5-8.5, but also major disagreements are identified (Figs. 7 and 8). Note that the median and interquartile ranges are only shown for ensembles that pass the limits with a probability of 50 % or more. For a good agreement between ensembles both probability and median needs to match. For the limit 2, the median value of exceedance agrees within 25 years and 1°C for ΔSAT, ΔAMOC, Southern Ocean Ω_a<1, Arctic Ocean Ω_a<1, Global Ocean Ω_a>3, and ΔPOM between the CMIP6 and the two EMIC ensembles. However, probability is variable among ensembles. The two EMIC ensembles generally show systematically high probability in limit exceedances in the first two limit sets (except limits 2 of UVic's ΔΦ and Bern3D Hypoxic ΔO_2) while the CMIP6 ensemble shows only 4 exceedances with medium probability over the same limits. The CMIP6 ensemble shows somewhat larger warming than the EMIC ensemble with earlier exceedance. This is consistent with the fact that the CMIP6 ensemble includes models with climate sensitivity larger than observation-constrained estimates (Nijsse et al., 2020; Tokarska et al., 2020). For the third and fourth limit sets, the CMIP6 models show medium

probability in the exceedance of the hypoxic ΔO_2, whereas the EMIC ensembles show no exceedance or with little probability. The finer spatial resolution used in CMIP6 models compared to the EMIC ensemble could explain this difference.

Regarding the uncertainties related to the exceedance of limits, the three ensemble agrees generally well over many metrics (Fig. 7). Regarding ΔPOM and hypoxic ΔO_2, the uncertainty range from the CMIP6 ensemble is larger than the EMIC ensembles. We hypothesize that the parametric uncertainty sampled in the perturbed-parameter EMIC ensembles is a significant underestimation of the full uncertainty signal of some metrics as it lacks the structural model uncertainty inherent in the CMIP6 ensemble. The ESMs' uncertainties of exceedances related to Southern Ocean $\Omega_a<1$, Arctic Ocean $\Omega_a<1$, Global Ocean $\Omega_a>3$ are narrower than the one from EMICs. We interpret this difference by an efficient bias correction of the present-day mean state applied to these metrics for CMIP6 ESMs.

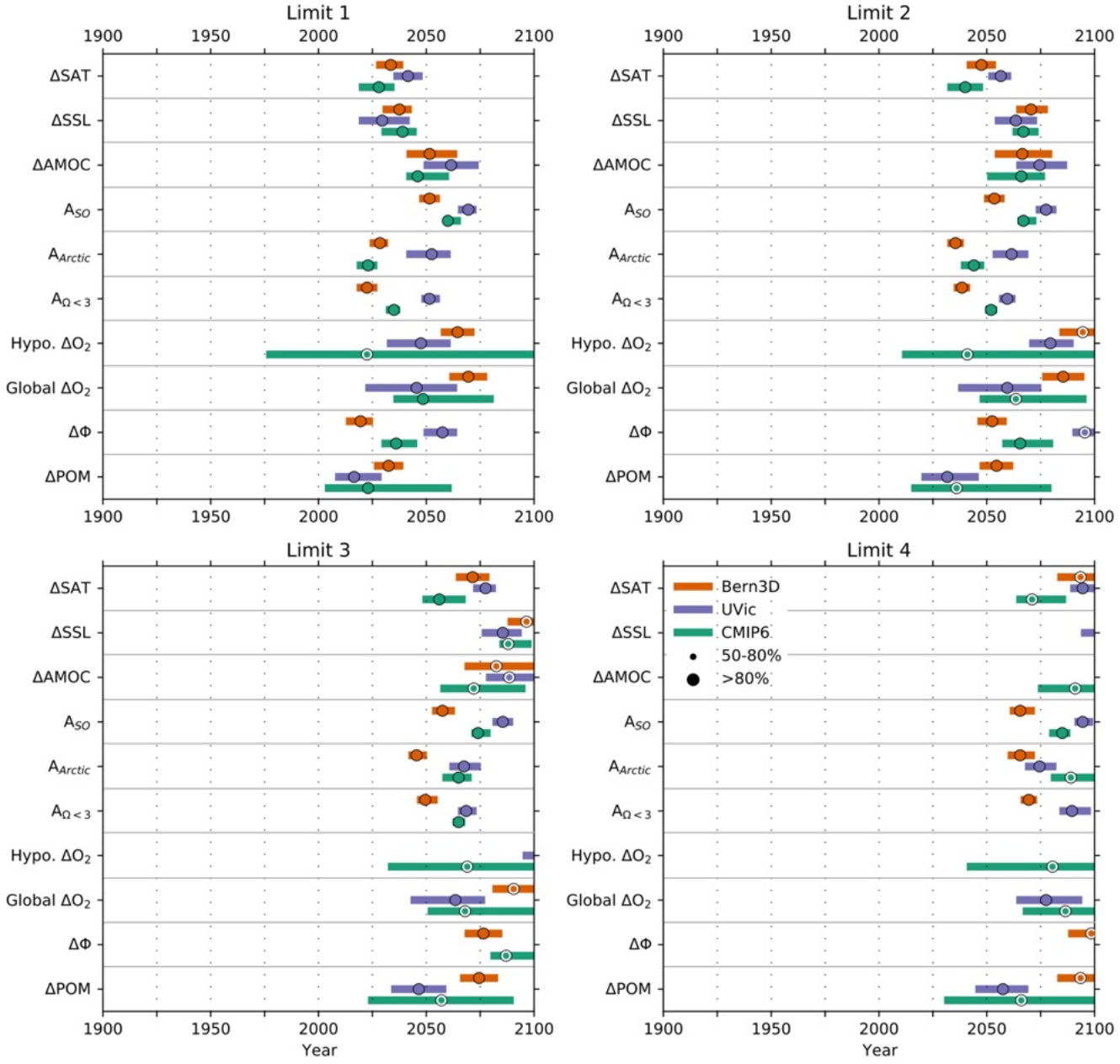

Figure 7: Box plots showing the interquartile range distribution of exceedance years for each mitigation limit of the impact metrics (abbreviations follow Table 1) for SSP5-8.5. Orange, purple, and green show data from the Bern3D-LPX, UVic, and CMIP6 ensemble, respectively. Dots indicate the median and the size of the dots indicates the percentage of ensemble members that have crossed the respective limit. The median and interquartile ranges are only shown for ensembles that pass the limits with a probability of 50 % or more. MHW, SIE, NPP and ΔBiomass are not shown because EMIC ensembles were not able to provide data for these metrics.

Despite such differences, robust conclusions emerge. First, both the CMIP6 and EMIC ensembles show medians passing most of the stringent limits of set 1 and set 2 with high probability within this century for global warming of 2.5°C and 3.5°C,

450 respectively (Fig. 8). Exceptions are ΔΦ, ΔSSL (known to lag surface warming and continues to increase over centuries), and ΔO_2 metrics, for which the CMIP6 and EMIC ensembles disagree. Second, both the CMIP6 and EMIC ensembles demonstrate that many less stringent limits of set 3 and set 4 are not passed with high probability within this century for global warming of 1.5°C and 2°C, respectively (Fig. 8). Taken together, the results of the model ensembles collectively show that limiting global warming below 2°C avoids passing the considered Earth system limits during this century with potentially dangerous impacts
455 on eco- and socio-economic systems.

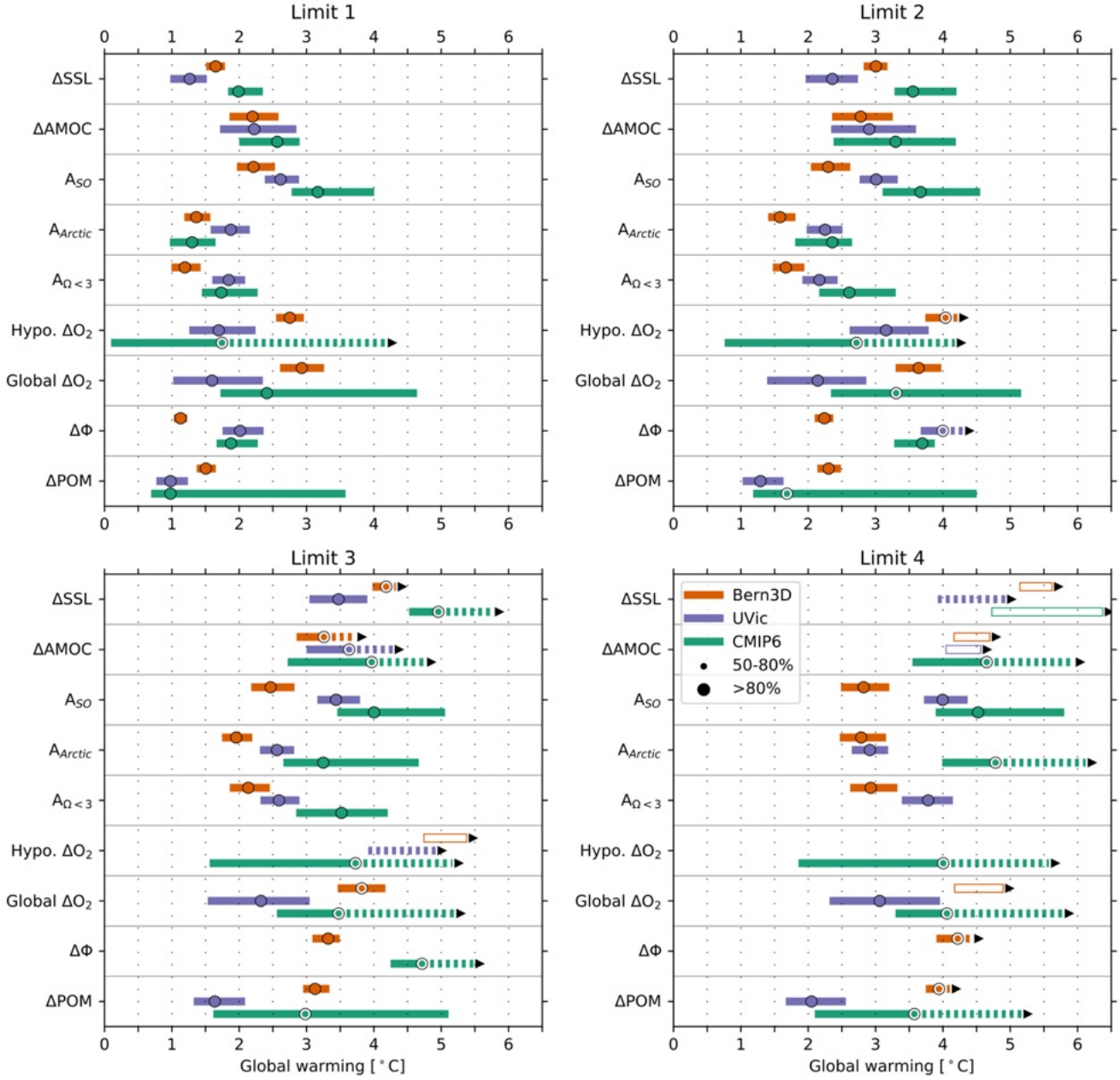

Figure 8: Same as Figure 7 but according to global warming following ΔSAT definition. Symbols and legends are following the same approach as in Figure 2.

4 Implications and Conclusion

This study assesses different types of IPCC emission pathways (low, high, overshoot) with respect to multi-dimensional safe operating spaces quantified by a wide range of physical, chemical, and biological ocean impact metrics and corresponding mitigation limits based on the literature. It contributes to identifying viable mitigation pathways for the 21st century projected by state-of-the-art Earth System Models, complemented by two observation-constrained ensembles from Earth System Models of Intermediate Complexity.

4.1 Limitations

Our study assesses a wide range of mitigation metrics over three very distinct scenario pathways and uses a large set of model results. Nevertheless, the global viewpoint that our study takes imposes certain limitations. Most important, the definitions of our metrics use averages over the global ocean or large oceanic regions neglecting spatial heterogeneity of changes in the climate system. For instance, while our metric Arctic Ocean $\Omega_a<1$ averages across the whole ocean north of 70°N, there is significant regional variability in the extent and rate of aragonite undersaturation across the Arctic Ocean. Areas with high freshwater input from sea ice melt, such as the Canadian Arctic Archipelago, experience more rapid acidification compared to regions influenced by Atlantic inflow, which have greater vertical mixing and primary production (Popova et al., 2014). Secondly, due to data limitations, we use only one ensemble member per ESM and scenario (many ESMs provide only one ensemble member). This is a limitation for metrics where changes in internal variability are important, as the marine heatwave metrics. For these metrics, the relative contributions of long-term warming trends versus anthropogenic changes in internal variability vary geographically, with the warming trend often accounting for more than 90% of the total changes (Deser et al., 2024; Frölicher et al., 2018; Frölicher and Laufkötter, 2018). By using a single simulation per model, we can provide a general assessment, but we fold together both model structural uncertainty and sampling uncertainty. To better assess MHW metrics under a moving-mean baseline, future studies should incorporate initial-condition large ensemble simulations (Burger et al., 2022; Deser et al., 2024), which would allow for a more robust evaluation of evolving forced responses in individual models at specific locations and times. Finally, for the metabolic index, we limited ourselves to illustrating the scenario- and model dependent changes in viable habitat based on metabolic traits for one median ecophysiotype (Fröb et al., 2024), while including a broader range of species' thermal and hypoxia sensitivities would allow for a broader multi-species assessment of habitability.

4.2 Physical changes

With these limitations in mind, we can draw several conclusions from our results, firstly for physical metrics. For SSL rise, models agree relatively well on the timing of when certain mitigation limits are crossed. Also, the value of stringent mitigation

is clearly visible in our results, since the less ambitious mitigation limits are only breached in the high emission scenario within this century. This also illustrates the value of late mitigation (compared to no mitigation) in the overshoot scenario, because also here the crossing of the two least ambitious limits is avoided. This is consistent with previous work showing that the rate of SSL rise is quite reversible in overshoot scenarios (Schwinger et al., 2022). It should be stressed, however, that sea level rise has a high inertia and will continue beyond the end-of-century time-horizon considered in this study, even in the strong mitigation scenarios.

Our results highlight committed severe risks for marine ecosystems related to summer Arctic sea ice retreat whatever the emissions scenario. Even the least ambitious mitigation limit (ice-free Artic during summer; September sea-ice extent < 10^6 km^2) is passed with medium probability (50-80% of models) in the low emission scenario. The summer Arctic sea ice reduction affects marine biota, particularly species like the Arctic cod, which are crucial for the diet of upper trophic level predators such as the black guillemot. This leads to changes in diet composition and increased nestling starvation rates among seabirds (Divoky et al., 2015). The decline in Arctic sea ice directly threatens the food security and cultural continuity of Indigenous Peoples. Many Arctic communities rely on sea ice for hunting and fishing, which are essential for their livelihoods. The sea ice loss disrupts these traditional practices, leading to food insecurity and cultural disruption (Huntington et al., 2022). Further, the decline in sea ice extent is opening new shipping routes, such as the Northern Sea Route, which connects North-East Asia with North-Western Europe. This route reduces shipping distances by approximately one-third compared to the Southern Sea Route. The opening of the Northern Sea Route could lead to significant economic benefits for global trade but raises geopolitical concerns and environmental pressures related to Arctic shipping and global supply chain reorganization (Bekkers et al., 2018).

AMOC decline in CMIP6 models has been shown to be relatively insensitive to the emission scenario, at least up to 2060 (Weijer et al. 2020). This is also reflected in our results, since the median exceedances of limits 1 (20% decline) and 2 (25% decline) are not very different for the strong mitigation scenario SSP1-2.6 (albeit with a somewhat lower probability) compared to SSP5-8.5 and SSP5-3.4. Nevertheless, the inter-model spread of projected AMOC decline remains large.

4.3 Ocean acidification

Results for the metrics related to ocean acidification show a high probability of crossing ambitious mitigation limits for the Arctic and the global ocean even in the low emission scenario SSP1-2.6 while the mitigation limits specific to the Southern Ocean are only crossed for the high emission scenario. Seen from a perspective of scenarios with prescribed atmospheric CO_2 concentration, the uncertainty in these results is small. However, consistent with the study of Terhaar et al. (2023), uncertainties increase considerably when relating the ocean acidification related metrics to a specific global warming level. Ocean acidification poses a severe threat to early life stages of calcifying organisms which can dominate surface water communities in polar regions, e.g. the polar pteropod (Limacina helicina antarctica), leading to shell dissolution and fragility, high mortality, and reduced recruitment (Bednaršek et al., 2012; Gardner et al., 2018). This is of major importance as the pteropods contribute significantly to the pelagic food web and carbon export fluxes in this region (Hauri et al., 2016). Aragonite undersaturation in

the Arctic region threatens calcifying organisms such as plankton and invertebrates, which depend on calcium carbonate for their structural integrity. This can lead to changes in the composition of the Arctic ecosystem, affecting both planktonic and benthic communities (Bates et al., 2013; Yamamoto-Kawai et al., 2009). At $\Omega<3$, the global ocean experiences widespread negative biological and ecological effects, including reduced survival, growth, and calcification in many marine species, especially those that build shells or skeletons from calcium carbonate (e.g., corals, molluscs, some plankton species; Kroeker et al., 2010). Together with long-term warming these can lead to declines in primary production and carbon export (Moore et al., 2018), resulting in lower fishery yields and reduced ecosystem productivity.

4.4 Biogeochemical and biological changes

Maybe not surprisingly, we find the largest uncertainties for the biogeochemical metrics such as the one related to $\underline{O_2}$, NPP, plankton biomass and POM. In all the scenarios used in our study, models do not agree on the projected sign of change of NPP while models agree on the projected decline of plankton biomass, albeit with significant uncertainties on the amplitude of this decline. These results are consistent with previous literature (Kwiatkowski et al., 2020; Tittensor et al., 2021). Change in NPP and biomass are influenced by complex interactions among nutrients, temperature, and ecosystem dynamics which is often beyond model capacity (Tagliabue et al., 2021). Regarding the metabolic index, viable habitat for marine organisms is lost if species-specific thresholds of metabolic demand and oxygen availability are crossed. Future projections show a decline in ocean habitability due to the combined threat of ocean warming and deoxygenation, leading to high extinction risk for polar species and loss of biological richness in the tropics (e.g., Penn and Deutsch, 2022).

4.5 Concluding remarks

Assessing the exceedance of mitigation limits for multiple impact metrics requires large model ensembles to obtain high-probability signals and corresponding uncertainties for the exceedance estimates (in years and global warming levels) linked to the projection pathways. Our analysis clearly indicates the need for better constraining and/or weighting the CMIP6 ensemble to reduce the large uncertainties found for exceedance estimates of many of the impact metrics. Simulations beyond year 2100 are needed to assess the long-term impacts of anthropogenic emissions, especially for the volume of hypoxic waters, global oxygen inventory, AMOC response, and steric sea level rise.

Our results show that ambitious mitigation limits will be exceeded with high or medium probability even if a low-emission pathway is followed, but that exceeding less ambitious mitigation limits associated with a higher risk for severe impacts is unlikely in a low-emission scenario. In contrast, under the high-emission scenario, many of the less ambitious and more risk-prone mitigation limits are exceeded with high to medium probability. The benefit of strong mitigation efforts in the overshoot pathway is clearly measurable as a decrease in the exceedance probability of the least ambitious and most risk-prone mitigation limits. Nevertheless, our analysis clearly indicates a risk of more severe impacts in the overshoot scenario compared to the strong mitigation scenario, particularly in the mid-term, highlighting the benefit of early mitigation strategies to avoid an overshoot scenario.

Appendix

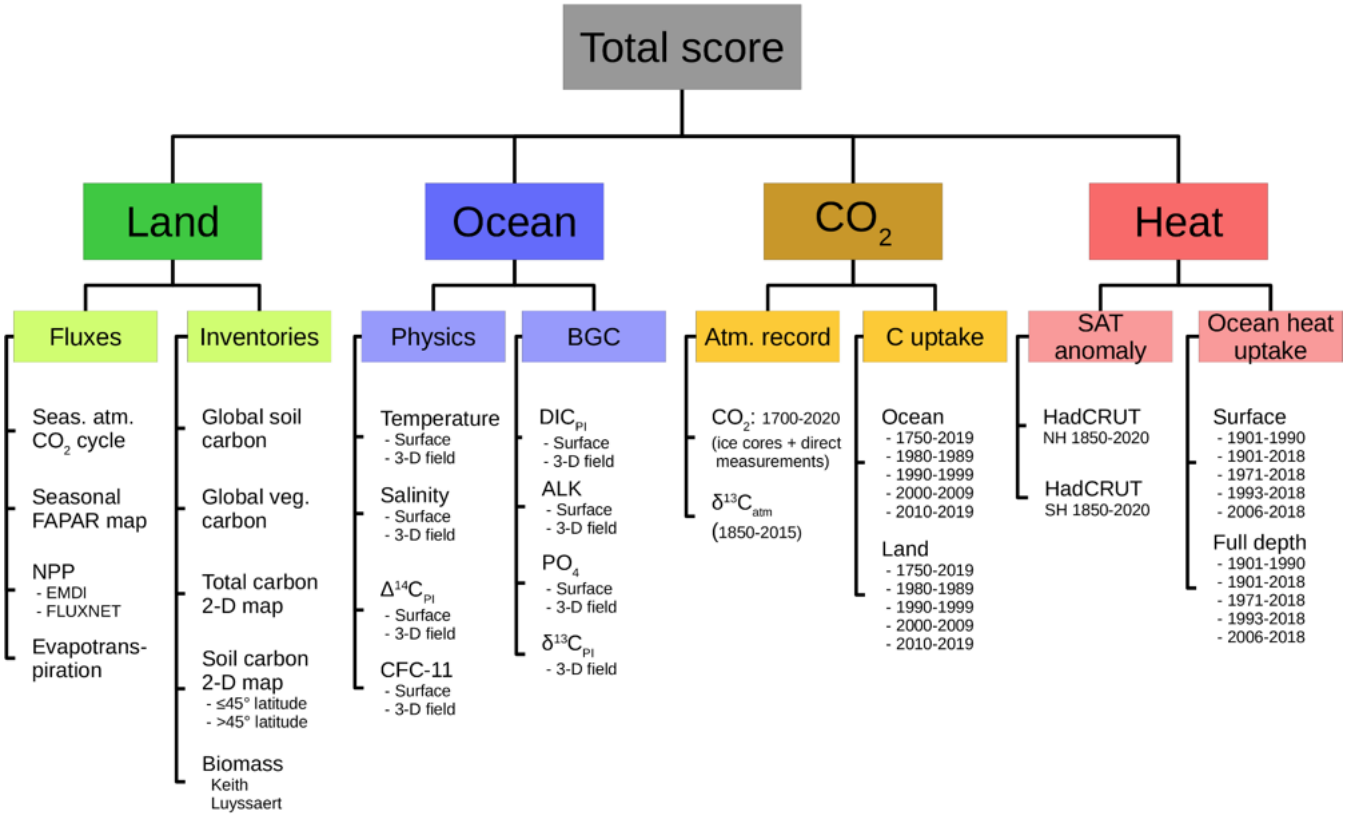

Figure A1: Hierarchical weighting scheme used to calculate the skill scores of individual ensemble members of the Bern3D-LPX model ensemble. Data sets at each level have equal weight. For example, the data-model mismatch in "Surface DIC" in the entry Ocean - BGC enters the total skill with a weight of 1/64 (½ (two data sets: Surface and 3-D field) x ¼ (4 groups: DIC, ALK, PO4, 13C) x ½ (two major subgroups: Physics, BGC) x ¼ (4 major groups: Land, Ocean, CO_2, Heat)).

UVic ESCM detailed methodology

A 325-member PPE is generated using a multi-wave history matching approach (Andrianakis et al., 2015; Bower et al., 2010). History matching (HM), or iterative refocusing, is based on running an ensemble in a predefined parameter space, using it to train statistical emulators that predict key metrics from the model output, and then using the emulator to identify the set of inputs that would give an acceptable match between the model output and the observed data. In our case, we performed six waves of 80 simulations each and compared model outputs with observations after each wave. Gaussian Process (GP) emulators (Kennedy and O'Hagan, 2001; Rasmussen and Williams, 2005; Sacks et al., 1989) are then constructed to predict these outputs as functions of the perturbed parameters to reject regions of the input space which are unlikely to produce results consistent with observations. For each quantity that we compare to observation, an implausibility measure (Andrianakis et al., 2015; Williamson et al., 2015) is computed following Eq. (1):

$$I_j(x) = \frac{|z_j - E^*[g_j(x)]|}{[V_o + V_c(x) + V_m]^{1/2}}, \quad (1)$$

where $g_j(x)$ is the function describing the relationship between a vector of model inputs x and a specific model output j. Since we employ GP emulation, we have the expectation provided by the emulators $E^*[g_j(x)]$. The corresponding observation is z_j. The term V_o, $V_c(x)$, and V_m represent the variance associated with the observational uncertainty, the code uncertainty as given by the emulator, and the model discrepancy. The latter is simply defined as 10 % of the ensemble range due to the difficulty to estimate model discrepancy. The value of I is large if it is unlikely for the model to produce an acceptable match with observation when using the input combination x. We adopt a similar approach as described in Jeltsch-Thömmes et al. (2024) for the Bern3D-LPX model to compute a score S based on our calculated implausibility measure $I_j(x)$. We generate a large Latin hypercube sampling plan and reject parameter combinations with emulated $I_j(x) > 3$. The emulated 1978-member ensemble was weighted using the score S and used for all statistical computations in this work.

To assess the quality of our GP emulators, we employ leave-one-out cross-validation. This validation is conducted using the surface air temperature anomaly (ΔSAT) relative to the preindustrial period, spanning the years 2015 to 2100. For our ensemble of 325 simulations, we iteratively exclude one simulation and construct an emulator of ΔSAT using the remaining 324 simulations. The emulator is then used to predict the ΔSAT of the omitted simulation. This process is repeated for each simulation in the ensemble, ensuring that every simulation is excluded once. Additionally, validation is performed at every 5th timestep in the time series.

Figure AX1 presents an example of the emulated versus simulated ΔSAT values at every 5-time steps for a randomly selected ensemble member. The error bars represent the two standard deviations of the predicted mean estimated by the emulator. For a well-calibrated emulator, approximately 95% of the true or simulated values should fall within 2 standard deviations of the emulated values.

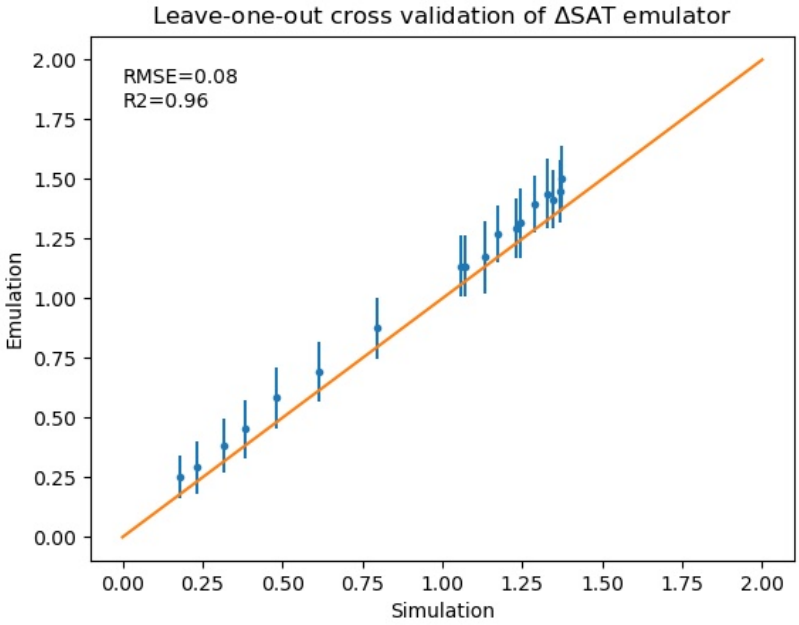

Figure AX1: Emulated value plotted against the simulated value for every 5th timestep (between 2014 and 2100) of a random ensemble member

595 We assess the emulator's performance using the root mean square error (RMSE) and the coefficient of determination (r^2), demonstrating that it effectively captures the behavior of the omitted simulation. Even though each time step is emulated independently and the temporal correlation between different timesteps are not known by the emulators, the whole emulated timeseries matches the simulated one well in this case (as indicated by the high r^2). A comprehensive summary of all validated timesteps across all simulations is shown in Figure AX2.

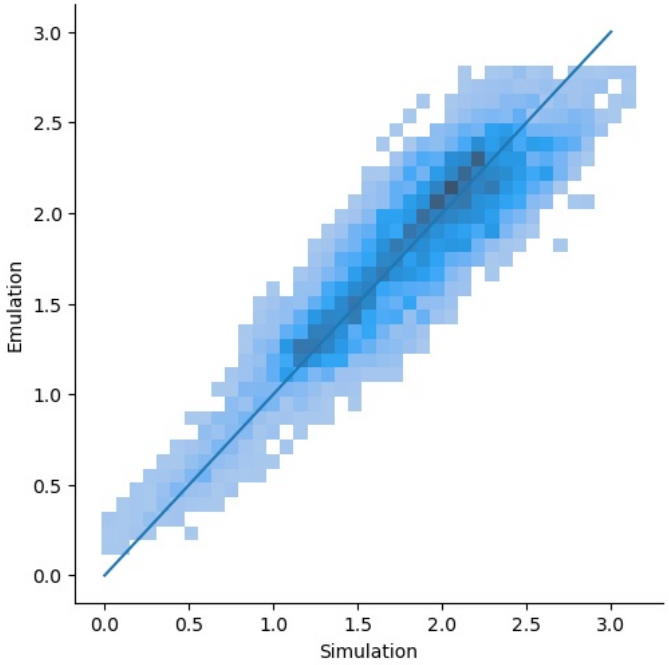

Figure AX2: Distribution of emulated versus simulated points

While some emulators exhibit lower performance, the vast majority produce emulated values that closely match the simulated ones. For each simulation, the RMSE is calculated for the time series and averaged across the entire ensemble, yielding a mean RMSE of 0.19°C, an error considered reasonable. The average coefficient of determination (r2) is 0.97, indicating also a strong agreement between the emulated and simulated values.

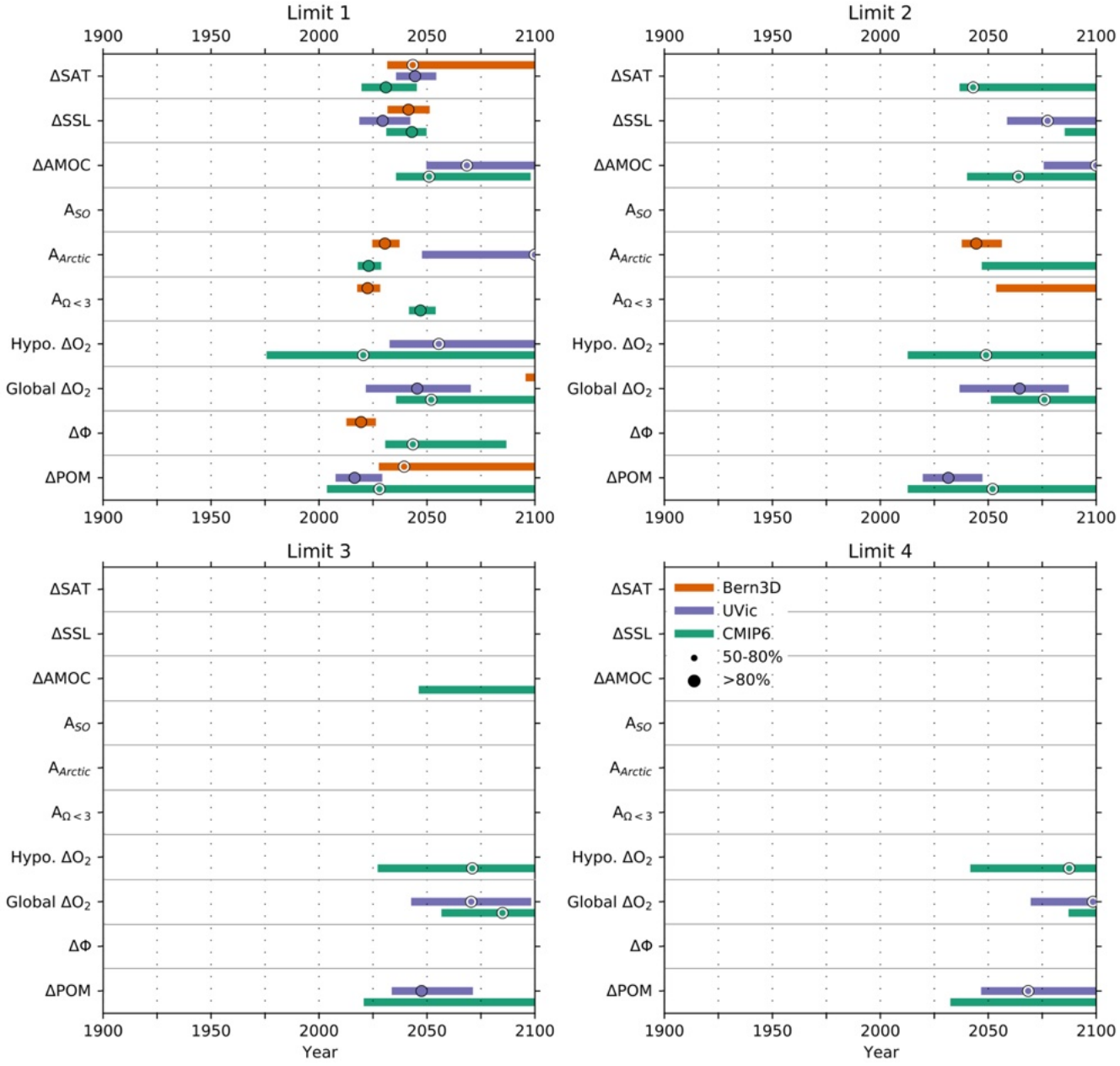

Figure A2: Same as in Figure 7 but for SSP1-2.6.

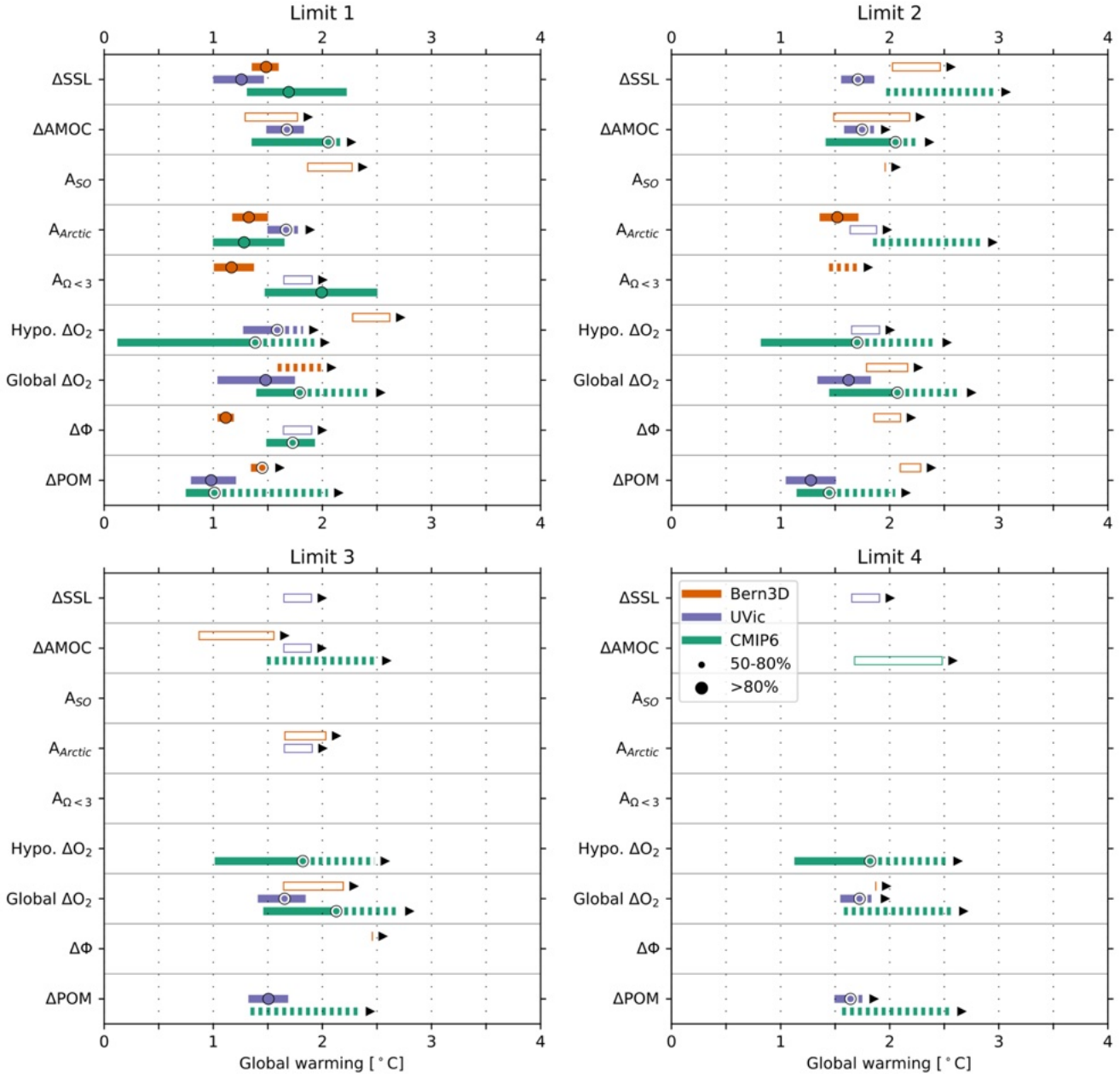

610 **Figure A3: Same as in Figure 8 but for SSP1-2.6.**

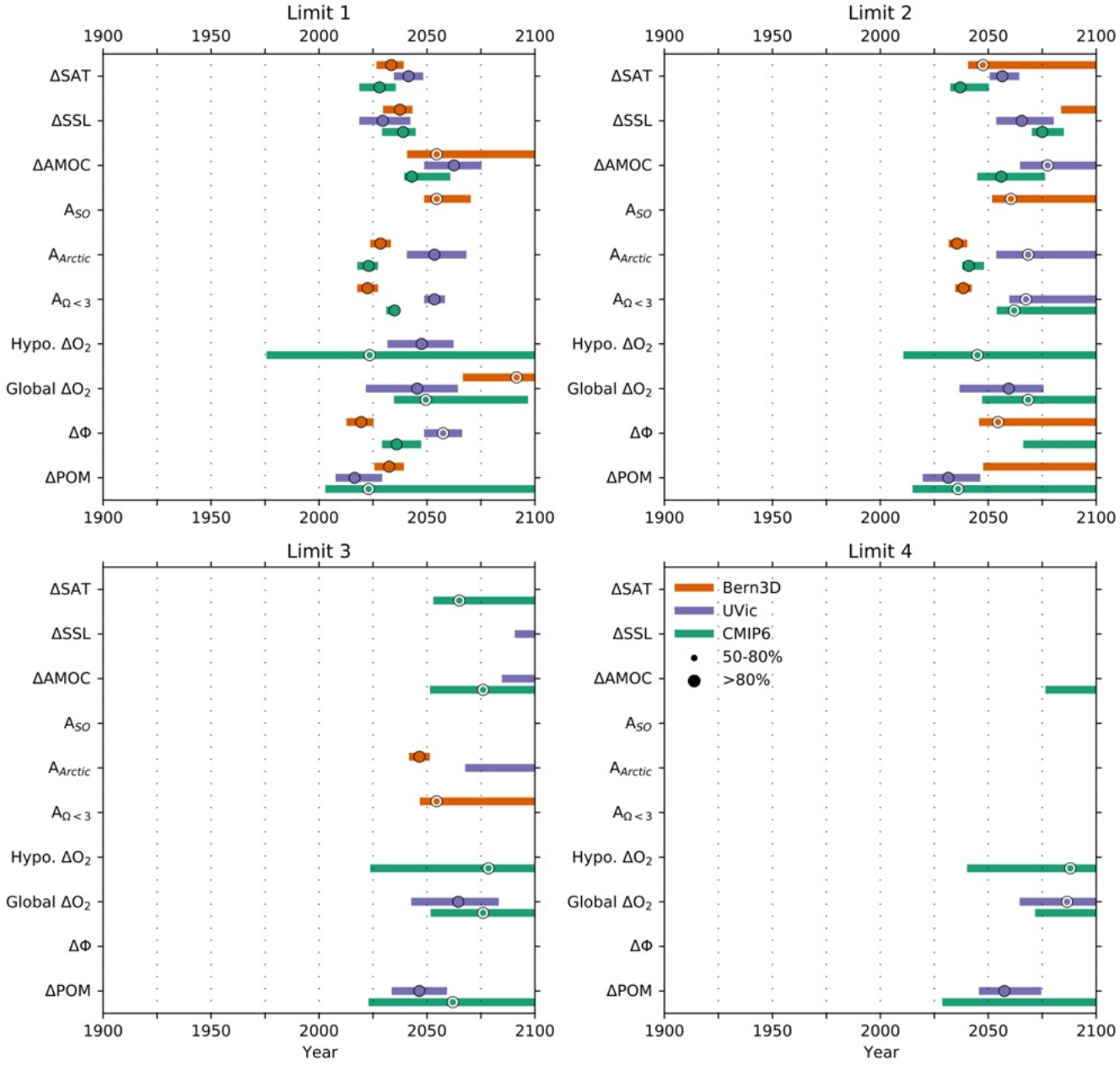

Figure A4: Same as in Figure 7 but for SSP5-3.4-OS.

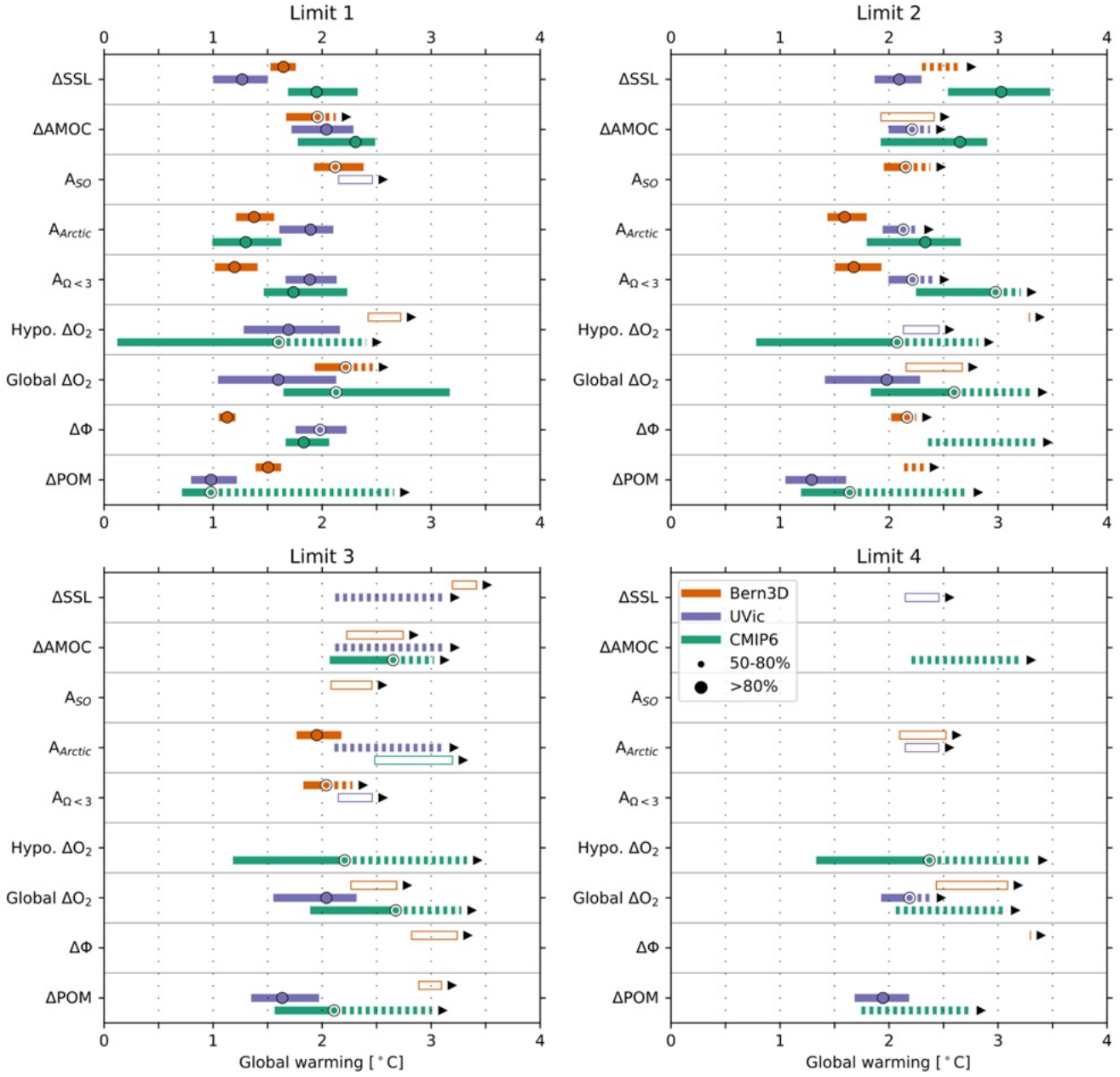

Figure A5: Same as in Figure 8 but for SSP5-3.4-OS.

Code availability

The mocsy 2.0 code is publicly available via https://github.com/jamesorr/mocsy (Orr and Epitalon, 2015).

Data availability

CMIP6 outputs are publicly available from the Earth System Grid Federation (ESGF) portals (e.g., https://esgf-data.dkrz.de/). The World Ocean Atlas 2013 (Locarnini et al., 2013; Zweng et al., 2013; https://www.nodc.noaa.gov/OC5/woa13/) and the GLODAPv2 (Lauvset et al., 2016; https://www.nodc.noaa.gov/ocads/oceans/GLODAPv2_2019/) data products are available from the National Oceanographic Data Center portal of the National Oceanic and Atmospheric Administration.

Author contribution

The study was led by T.B. who performed the CMIP6 calculations, analysis, and figures. O.T. processed the CMIP6 model data (download, regridding). F.F. provided the CMIP6 metabolic index data. A. J.-T. analysed the Bern-3D data and provided the EMICs figures. G. T. T. led the metrics' and limits' literature review and analysed the UVic data. T. L. F. provided the CMIP6 marine heatwave data. J. N. provided the summary Figs. 5 and 6. All authors were involved in designing the analysis, interpreting the results and writing the manuscript.

Competing interests

The authors declare that they have no conflict of interest.

Disclaimer

The work reflects only the authors' view; the European Commission and their executive agency are not responsible for any use that may be made of the information the work contains.

Acknowledgments

We acknowledge the World Climate Research Programme, which, through its Working Group on Coupled Modelling, coordinated and promoted CMIP. We thank the climate modelling groups for producing and making available their model output, the Earth System Grid Federation (ESGF) for archiving the data and providing access, and the multiple funding agencies who support CMIP and ESGF. All authors received funding from the European Union's Horizon 2020 research and innovation programme under grant agreement No. 820989 (COMFORT). TB and JS received also funding from the European Union's Horizon Europe research and innovation programme under grant agreement No. 869357 (OceanNETs). FJ and AJ acknowledge additional funding by the Swiss National Science Foundation (#200020_200511). TLF and FF received also funding from the European Union's Horizon Europe research and innovation programme under grant agreement No.

101137673 (TipESM). We also thank the IPSL modelling group for the software infrastructure, which facilitated CMIP6 analysis. We thank NORCE Research and the Bjerknes Centre for Climate Research for covering article processing charges.

References

Anderson, S. I., Barton, A. D., Clayton, S., Dutkiewicz, S., and Rynearson, T. A.: Marine phytoplankton functional types exhibit diverse responses to thermal change, Nat Commun, 12, 6413, https://doi.org/10.1038/s41467-021-26651-8, 2021.

Andrianakis, I., Vernon, I. R., McCreesh, N., McKinley, T. J., Oakley, J. E., Nsubuga, R. N., Goldstein, M., and White, R. G.: Bayesian History Matching of Complex Infectious Disease Models Using Emulation: A Tutorial and a Case Study on HIV in Uganda, PLOS Computational Biology, 11, e1003968, https://doi.org/10.1371/journal.pcbi.1003968, 2015.

Armstrong McKay, D. I., Staal, A., Abrams, J. F., Winkelmann, R., Sakschewski, B., Loriani, S., Fetzer, I., Cornell, S. E., Rockström, J., and Lenton, T. M.: Exceeding 1.5°C global warming could trigger multiple climate tipping points, Science, 377, eabn7950, https://doi.org/10.1126/science.abn7950, 2022.

Balvanera, P., Brauman, K. A., Cord, A. F., Drakou, E. G., Geijzendorffer, I. R., Karp, D. S., Martín-López, B., Mwampamba, T. H., and Schröter, M.: Essential ecosystem service variables for monitoring progress towards sustainability, Current Opinion in Environmental Sustainability, 54, 101152, https://doi.org/10.1016/j.cosust.2022.101152, 2022.

Bates, N. R., Orchowska, M. I., Garley, R., and Mathis, J. T.: Summertime calcium carbonate undersaturation in shelf waters of the western Arctic Ocean – how biological processes exacerbate the impact of ocean acidification, Biogeosciences, 10, 5281–5309, https://doi.org/10.5194/bg-10-5281-2013, 2013.

Battaglia, G. and Joos, F.: Hazards of decreasing marine oxygen: the near-term and millennial-scale benefits of meeting the Paris climate targets, Earth System Dynamics, 9, 797–816, https://doi.org/10.5194/esd-9-797-2018, 2018.

Battaglia, G., Steinacher, M., and Joos, F.: A probabilistic assessment of calcium carbonate export and dissolution in the modern ocean, Biogeosciences, 13, 2823–2848, https://doi.org/10.5194/bg-13-2823-2016, 2016.

Bednaršek, N., Tarling, G. A., Bakker, D. C. E., Fielding, S., Jones, E. M., Venables, H. J., Ward, P., Kuzirian, A., Lézé, B., Feely, R. A., and Murphy, E. J.: Extensive dissolution of live pteropods in the Southern Ocean, Nature Geosci, 5, 881–885, https://doi.org/10.1038/ngeo1635, 2012.

Bekkers, E., Francois, J. F., and Rojas-Romagosa, H.: Melting ice Caps and the Economic Impact of Opening the Northern Sea Route, The Economic Journal, 128, 1095–1127, https://doi.org/10.1111/ecoj.12460, 2018.

Bitz, C. M., Holland, M. M., Weaver, A. J., and Eby, M.: Simulating the ice-thickness distribution in a coupled climate model, Journal of Geophysical Research: Oceans, 106, 2441–2463, https://doi.org/10.1029/1999JC000113, 2001.

Bopp, L., Resplandy, L., Orr, J. C., Doney, S. C., Dunne, J. P., Gehlen, M., Halloran, P., Heinze, C., Ilyina, T., Séférian, R., Tjiputra, J., and Vichi, M.: Multiple stressors of ocean ecosystems in the 21st century: projections with CMIP5 models, Biogeosciences, 10, 6225–6245, https://doi.org/10.5194/bg-10-6225-2013, 2013.

Bopp, L., Aumont, O., Kwiatkowski, L., Clerc, C., Dupont, L., Ethé, C., Gorgues, T., Séférian, R., and Tagliabue, A.: Diazotrophy as a key driver of the response of marine net primary productivity to climate change, Biogeosciences, 19, 4267–4285, https://doi.org/10.5194/bg-19-4267-2022, 2022.

Boucher, O., Halloran, P. R., Burke, E. J., Doutriaux-Boucher, M., Jones, C. D., Lowe, J., Ringer, M. A., Robertson, E., and Wu, P.: Reversibility in an Earth System model in response to CO_2 concentration changes, Environ. Res. Lett., 7, 024013, https://doi.org/10.1088/1748-9326/7/2/024013, 2012.

Boucher, O., Servonnat, J., Albright, A. L., Aumont, O., Balkanski, Y., Bastrikov, V., Bekki, S., Bonnet, R., Bony, S., Bopp, L., Braconnot, P., Brockmann, P., Cadule, P., Caubel, A., Cheruy, F., Codron, F., Cozic, A., Cugnet, D., D'Andrea, F., Davini, P., de Lavergne, C., Denvil, S., Deshayes, J., Devilliers, M., Ducharne, A., Dufresne, J., Dupont, E., Éthé, C., Fairhead, L., Falletti, L., Flavoni, S., Foujols, M., Gardoll, S., Gastineau, G., Ghattas, J., Grandpeix, J., Guenet, B., Guez, L., E., Guilyardi, E., Guimberteau, M., Hauglustaine, D., Hourdin, F., Idelkadi, A., Joussaume, S., Kageyama, M., Khodri, M., Krinner, G., Lebas, N., Levavasseur, G., Lévy, C., Li, L., Lott, F., Lurton, T., Luyssaert, S., Madec, G., Madeleine, J., Maignan, F., Marchand, M., Marti, O., Mellul, L., Meurdesoif, Y., Mignot, J., Musat, I., Ottlé, C., Peylin, P., Planton, Y., Polcher, J., Rio, C., Rochetin, N., Rousset, C., Sepulchre, P., Sima, A., Swingedouw, D., Thiéblemont, R., Traore, A. K., Vancoppenolle, M., Vial, J., Vialard, J., Viovy, N., and Vuichard, N.: Presentation and Evaluation of the IPSL-CM6A-LR Climate Model, J Adv Model Earth Syst, 12, https://doi.org/10.1029/2019MS002010, 2020.

Bower, R. G., Goldstein, M., and Vernon, I.: Galaxy formation: a Bayesian uncertainty analysis, Bayesian Analysis, 5, 619–669, https://doi.org/10.1214/10-BA524, 2010.

Burger, F. A., Terhaar, J., and Frölicher, T. L.: Compound marine heatwaves and ocean acidity extremes, Nat Commun, 13, 4722, https://doi.org/10.1038/s41467-022-32120-7, 2022.

Canadell, J. G., Monteiro, P. M. S., Costa, M. H., Cotrim da Cunha, L., Cox, P. M., Eliseev, A. V., Henson, S., Ishii, M., Jaccard, S., Koven, C., Lohila, A., Patra, P. K., Piao, S., Rogelj, J., Syampungani, S., Zaehle, S., and Zickfeld, K.: Global Carbon and other Biogeochemical Cycles and Feedbacks, edited by: Masson-Delmotte, V., Zhai, P., Pirani, A., Connors, S. L., Péan, C., Berger, S., Caud, N., Chen, Y., Goldfarb, L., Gomis, M. I., Huang, M., Leitzell, K., Lonnoy, E., Matthews, J. B. R., Maycock, T. K., Waterfield, T., Yelekçi, O., Yu, R., and Zhou, B., Climate Change 2021: The Physical Science Basis. Contribution of Working Group I to the Sixth Assessment Report of the Intergovernmental Panel on Climate Change, https://doi.org/10.1017/9781009157896.007, 2021.

Capotondi, A., Rodrigues, R. R., Sen Gupta, A., Benthuysen, J. A., Deser, C., Frölicher, T. L., Lovenduski, N. S., Amaya, D. J., Le Grix, N., Xu, T., Hermes, J., Holbrook, N. J., Martinez-Villalobos, C., Masina, S., Roxy, M. K., Schaeffer, A., Schlegel, R. W., Smith, K. E., and Wang, C.: A global overview of marine heatwaves in a changing climate, Commun Earth Environ, 5, 701, https://doi.org/10.1038/s43247-024-01806-9, 2024.

Chen, D., Rojas, M., Samset, B. H., Cobb, K., Diongue Niang, A., Edwards, P., Emori, S., Faria, S. H., Hawkins, E., Hope, P., Huybrechts, P., Meinshausen, M., Mustafa, S. K., Plattner, G.-K., and Tréguier, A.-M.: Framing, Context, and Methods, edited by: Masson-Delmotte, V., Zhai, P., Pirani, A., Connors, S. L., Péan, C., Berger, S., Caud, N., Chen, Y., Goldfarb, L., Gomis, M. I., Huang, M., Leitzell, K., Lonnoy, E., Matthews, J. B. R., Maycock, T. K., Waterfield, T., Yelekçi, O., Yu, R., and Zhou, B., Climate Change 2021: The Physical Science Basis. Contribution of Working Group I to the Sixth Assessment Report of the Intergovernmental Panel on Climate Change, https://doi.org/10.1017/9781009157896.003, 2021.

Cherchi, A., Fogli, P. G., Lovato, T., Peano, D., Iovino, D., Gualdi, S., Masina, S., Scoccimarro, E., Materia, S., Bellucci, A., and Navarra, A.: Global Mean Climate and Main Patterns of Variability in the CMCC-CM2 Coupled Model, Journal of Advances in Modeling Earth Systems, 11, 185–209, https://doi.org/10.1029/2018MS001369, 2019.

Church, J., Gregory, J., White, N., Platten, S., and Mitrovica, J.: Understanding and Projecting Sea Level Change, Oceanog., 24, 130–143, https://doi.org/10.5670/oceanog.2011.33, 2011.

Cocco, V., Joos, F., Steinacher, M., Frölicher, T. L., Bopp, L., Dunne, J., Gehlen, M., Heinze, C., Orr, J., Oschlies, A., Schneider, B., Segschneider, J., and Tjiputra, J.: Oxygen and indicators of stress for marine life in multi-model global warming projections, Biogeosciences, 10, 1849–1868, https://doi.org/10.5194/bg-10-1849-2013, 2013.

Danabasoglu, G., Lamarque, J. -F., Bacmeister, J., Bailey, D. A., DuVivier, A. K., Edwards, J., Emmons, L. K., Fasullo, J., Garcia, R., Gettelman, A., Hannay, C., Holland, M. M., Large, W. G., Lauritzen, P. H., Lawrence, D. M., Lenaerts, J. T. M., Lindsay, K., Lipscomb, W. H., Mills, M. J., Neale, R., Oleson, K. W., Otto-Bliesner, B., Phillips, A. S., Sacks, W., Tilmes, S., Kampenhout, L., Vertenstein, M., Bertini, A., Dennis, J., Deser, C., Fischer, C., Fox-Kemper, B., Kay, J. E., Kinnison, D., Kushner, P. J., Larson, V. E., Long, M. C., Mickelson, S., Moore, J. K., Nienhouse, E., Polvani, L., Rasch, P. J., and Strand, W. G.: The Community Earth System Model Version 2 (CESM2), J. Adv. Model. Earth Syst., 12, https://doi.org/10.1029/2019MS001916, 2020.

Deser, C., Phillips, A. S., Alexander, Michael. A., Amaya, D. J., Capotondi, A., Jacox, M. G., and Scott, J. D.: Future Changes in the Intensity and Duration of Marine Heat and Cold Waves: Insights from Coupled Model Initial-Condition Large Ensembles, Journal of Climate, 37, 1877–1902, https://doi.org/10.1175/JCLI-D-23-0278.1, 2024.

Deutsch, C., Ferrel, A., Seibel, B., Pörtner, H.-O., and Huey, R. B.: Climate change tightens a metabolic constraint on marine habitats, Science, 348, 1132–1135, https://doi.org/10.1126/science.aaa1605, 2015.

Deutsch, C., Penn, J. L., and Seibel, B.: Metabolic trait diversity shapes marine biogeography, Nature, 585, 557–562, https://doi.org/10.1038/s41586-020-2721-y, 2020.

Diaz, R. J. and Rosenberg, R.: Spreading Dead Zones and Consequences for Marine Ecosystems, Science, 321, 926–929, https://doi.org/10.1126/science.1156401, 2008.

Divoky, G. J., Lukacs, P. M., and Druckenmiller, M. L.: Effects of recent decreases in arctic sea ice on an ice-associated marine bird, Progress in Oceanography, 136, 151–161, https://doi.org/10.1016/j.pocean.2015.05.010, 2015.

Doney, S. C., Fabry, V. J., Feely, R. A., and Kleypas, J. A.: Ocean Acidification: The Other CO2 Problem, Annu. Rev. Mar. Sci., 1, 169–192, https://doi.org/10.1146/annurev.marine.010908.163834, 2009.

Doney, S. C., Busch, D. S., Cooley, S. R., and Kroeker, K. J.: The Impacts of Ocean Acidification on Marine Ecosystems and Reliant Human Communities, Annu. Rev. Environ. Resour., 45, 83–112, https://doi.org/10.1146/annurev-environ-012320-083019, 2020.

Dutkiewicz, S., Scott, J. R., and Follows, M. J.: Winners and losers: Ecological and biogeochemical changes in a warming ocean, Global Biogeochem. Cycles, 27, 463–477, https://doi.org/10.1002/gbc.20042, 2013.

Edwards, N. R., Willmott, A. J., and Killworth, P. D.: On the Role of Topography and Wind Stress on the Stability of the Thermohaline Circulation, Journal of Physical Oceanography, 28, 756–778, https://doi.org/10.1175/1520-0485(1998)028<0756:OTROTA>2.0.CO;2, 1998.

Ekau, W., Auel, H., Pörtner, H.-O., and Gilbert, D.: Impacts of hypoxia on the structure and processes in pelagic communities (zooplankton, macro-invertebrates and fish), Biogeosciences, 7, 1669–1699, https://doi.org/10.5194/bg-7-1669-2010, 2010.

Ekstrom, J. A., Suatoni, L., Cooley, S. R., Pendleton, L. H., Waldbusser, G. G., Cinner, J. E., Ritter, J., Langdon, C., Van Hooidonk, R., Gledhill, D., Wellman, K., Beck, M. W., Brander, L. M., Rittschof, D., Doherty, C., Edwards, P. E. T., and Portela, R.: Vulnerability and adaptation of US shellfisheries to ocean acidification, Nature Clim Change, 5, 207–214, https://doi.org/10.1038/nclimate2508, 2015.

Enting, I. G.: On the use of smoothing splines to filter CO_2 data, J. Geophys. Res., 92, 10977–10984, https://doi.org/10.1029/JD092iD09p10977, 1987.

Fabry, V., McClintock, J., Mathis, J., and Grebmeier, J.: Ocean Acidification at High Latitudes: The Bellwether, Oceanog., 22, 160–171, https://doi.org/10.5670/oceanog.2009.105, 2009.

Fanning, A. F. and Weaver, A. J.: An atmospheric energy-moisture balance model: Climatology, interpentadal climate change, and coupling to an ocean general circulation model, J. Geophys. Res., 101, 15111–15128, https://doi.org/10.1029/96JD01017, 1996.

Fox-Kemper, B., Hewitt, H. T., Xiao, C., Aðalgeirsdóttir, G., Drijfhout, S. S., Edwards, T. L., Golledge, N. R., Hemer, M., Kopp, R. E., Krinner, G., Mix, A., Notz, D., Nowicki, S., Nurhati, I. S., Ruiz, L., Sallée, J.-B., Slangen, A. B. A., and Yu, Y.: Ocean, Cryosphere and Sea Level Change, in: Climate Change 2021: The Physical Science Basis. Contribution of Working Group I to the Sixth Assessment Report of the Intergovernmental Panel on Climate Change, edited by: Masson-Delmotte, V., Zhai, P., Pirani, A., Connors, S. L., Péan, C., Berger, S., Caud, N., Chen, Y., Goldfarb, L., Gomis, M. I., Huang, M., Leitzell, K., Lonnoy, E., Matthews, J. B. R., Maycock, T. K., Waterfield, T., Yelekçi, O., Yu, R., and Zhou, B., Cambridge University Press, Cambridge, UK and New York, NY, USA, https://doi.org/10.1017/9781009157896.011, 2021.

Fröb, F., Bourgeois, T., Goris, N., Schwinger, J., and Heinze, C.: Simulated Abrupt Shifts in Aerobic Habitats of Marine Species in the Past, Present, and Future, Earth's Future, 12, e2023EF004141, https://doi.org/10.1029/2023EF004141, 2024.

Frölicher, T. L. and Laufkötter, C.: Emerging risks from marine heat waves, Nat Commun, 9, 650, https://doi.org/10.1038/s41467-018-03163-6, 2018.

Frölicher, T. L., Rodgers, K. B., Stock, C. A., and Cheung, W. W. L.: Sources of uncertainties in 21st century projections of potential ocean ecosystem stressors, Global Biogeochemical Cycles, 30, 1224–1243, https://doi.org/10.1002/2015GB005338, 2016.

Frölicher, T. L., Fischer, E. M., and Gruber, N.: Marine heatwaves under global warming, Nature, 560, 360–364, https://doi.org/10.1038/s41586-018-0383-9, 2018.

Fu, W., Randerson, J. T., and Moore, J. K.: Climate change impacts on net primary production (NPP) and export production(EP) regulated by increasing stratification and phytoplankton communitystructure in the CMIP5 models, Biogeosciences, 13, 5151–5170, https://doi.org/10.5194/bg-13-5151-2016, 2016.

Gardner, J., Manno, C., Bakker, D. C. E., Peck, V. L., and Tarling, G. A.: Southern Ocean pteropods at risk from ocean warming and acidification, Mar Biol, 165, 8, https://doi.org/10.1007/s00227-017-3261-3, 2018.

Gattuso, J.-P., Magnan, A., Billé, R., Cheung, W. W. L., Howes, E. L., Joos, F., Allemand, D., Bopp, L., Cooley, S. R., Eakin, C. M., Hoegh-Guldberg, O., Kelly, R. P., Pörtner, H.-O., Rogers, A. D., Baxter, J. M., Laffoley, D., Osborn, D., Rankovic, A., Rochette, J., Sumaila, U. R., Treyer, S., and Turley, C.: Contrasting futures for ocean and society from different anthropogenic CO2 emissions scenarios, Science, 349, aac4722, https://doi.org/10.1126/science.aac4722, 2015.

Gazeau, F., Quiblier, C., Jansen, J. M., Gattuso, J., Middelburg, J. J., and Heip, C. H. R.: Impact of elevated CO_2 on shellfish calcification, Geophysical Research Letters, 34, 2006GL028554, https://doi.org/10.1029/2006GL028554, 2007.

Gimenez, I., Waldbusser, G. G., and Hales, B.: Ocean acidification stress index for shellfish (OASIS): Linking Pacific oyster larval survival and exposure to variable carbonate chemistry regimes, Elementa: Science of the Anthropocene, 6, 51, https://doi.org/10.1525/elementa.306, 2018.

Gruber, N.: Warming up, turning sour, losing breath: ocean biogeochemistry under global change, Phil. Trans. R. Soc. A., 369, 1980–1996, https://doi.org/10.1098/rsta.2011.0003, 2011.

Guinotte, J. M., Buddemeier, R. W., and Kleypas, J. A.: Future coral reef habitat marginality: temporal and spatial effects of climate change in the Pacific basin, Coral Reefs, 22, 551–558, https://doi.org/10.1007/s00338-003-0331-4, 2003.

Guinotte, J. M., Orr, J., Cairns, S., Freiwald, A., Morgan, L., and George, R.: Will human-induced changes in seawater chemistry alter the distribution of deep-sea scleractinian corals?, Frontiers in Ecology and the Environment, 4, 141–146, https://doi.org/10.1890/1540-9295(2006)004[0141:WHCISC]2.0.CO;2, 2006.

Hague, B. S., McGregor, S., Jones, D. A., Reef, R., Jakob, D., and Murphy, B. F.: The Global Drivers of Chronic Coastal Flood Hazards Under Sea-Level Rise, Earth's Future, 11, e2023EF003784, https://doi.org/10.1029/2023EF003784, 2023.

Hajima, T., Watanabe, M., Yamamoto, A., Tatebe, H., Noguchi, M. A., Abe, M., Ohgaito, R., Ito, A., Yamazaki, D., Okajima, H., Ito, A., Takata, K., Ogochi, K., Watanabe, S., and Kawamiya, M.: Development of the MIROC-ES2L Earth system model and the evaluation of biogeochemical processes and feedbacks, Geosci. Model Dev., 13, 2197–2244, https://doi.org/10.5194/gmd-13-2197-2020, 2020.

Hameau, A., Frölicher, T. L., Mignot, J., and Joos, F.: Is deoxygenation detectable before warming in the thermocline?, Biogeosciences, 17, 1877–1895, https://doi.org/10.5194/bg-17-1877-2020, 2020.

Hauri, C., Friedrich, T., and Timmermann, A.: Abrupt onset and prolongation of aragonite undersaturation events in the Southern Ocean, Nature Clim Change, 6, 172–176, https://doi.org/10.1038/nclimate2844, 2016.

Heinze, C., Blenckner, T., Martins, H., Rusiecka, D., Döscher, R., Gehlen, M., Gruber, N., Holland, E., Hov, Ø., Joos, F., Matthews, J. B. R., Rødven, R., and Wilson, S.: The quiet crossing of ocean tipping points, Proc. Natl. Acad. Sci. U.S.A., 118, e2008478118, https://doi.org/10.1073/pnas.2008478118, 2021.

Hermans, T. H. J., Gregory, J. M., Palmer, M. D., Ringer, M. A., Katsman, C. A., and Slangen, A. B. A.: Projecting Global Mean Sea-Level Change Using CMIP6 Models, Geophysical Research Letters, 48, https://doi.org/10.1029/2020GL092064, 2021.

Hinkel, J., Lincke, D., Vafeidis, A. T., Perrette, M., Nicholls, R. J., Tol, R. S. J., Marzeion, B., Fettweis, X., Ionescu, C., and Levermann, A.: Coastal flood damage and adaptation costs under 21st century sea-level rise, Proc. Natl. Acad. Sci. U.S.A., 111, 3292–3297, https://doi.org/10.1073/pnas.1222469111, 2014.

Hoegh-Guldberg, O., Mumby, P. J., Hooten, A. J., Steneck, R. S., Greenfield, P., Gomez, E., Harvell, C. D., Sale, P. F., Edwards, A. J., Caldeira, K., Knowlton, N., Eakin, C. M., Iglesias-Prieto, R., Muthiga, N., Bradbury, R. H., Dubi, A., and Hatziolos, M. E.: Coral Reefs Under Rapid Climate Change and Ocean Acidification, Science, 318, 1737–1742, https://doi.org/10.1126/science.1152509, 2007.

Hunke, E. C. and Dukowicz, J. K.: An Elastic–Viscous–Plastic Model for Sea Ice Dynamics, J. Phys. Oceanogr., 27, 1849–1867, https://doi.org/10.1175/1520-0485(1997)027<1849:AEVPMF>2.0.CO;2, 1997.

Huntington, H. P., Zagorsky, A., Kaltenborn, B. P., Shin, H. C., Dawson, J., Lukin, M., Dahl, P. E., Guo, P., and Thomas, D. N.: Societal implications of a changing Arctic Ocean, Ambio, 51, 298–306, https://doi.org/10.1007/s13280-021-01601-2, 2022.

Jackson, L. C., Biastoch, A., Buckley, M. W., Desbruyères, D. G., Frajka-Williams, E., Moat, B., and Robson, J.: The evolution of the North Atlantic Meridional Overturning Circulation since 1980, Nat Rev Earth Environ, 3, 241–254, https://doi.org/10.1038/s43017-022-00263-2, 2022.

Jeltsch-Thömmes, A., Stocker, T. F., and Joos, F.: Hysteresis of the Earth system under positive and negative CO_2 emissions, Environ. Res. Lett., 15, 124026, https://doi.org/10.1088/1748-9326/abc4af, 2020.

Jeltsch-Thömmes, A., Tran, G., Lienert, S., Keller, D. P., Oschlies, A., and Joos, F.: Earth system responses to carbon dioxide removal as exemplified by ocean alkalinity enhancement: tradeoffs and lags, Environ. Res. Lett., 19, 054054, https://doi.org/10.1088/1748-9326/ad4401, 2024.

Keller, D. P., Oschlies, A., and Eby, M.: A new marine ecosystem model for the University of Victoria Earth System Climate Model, Geoscientific Model Development, 5, 1195–1220, https://doi.org/10.5194/gmd-5-1195-2012, 2012.

Kennedy, M. C. and O'Hagan, A.: Bayesian calibration of computer models, Journal of the Royal Statistical Society: Series B (Statistical Methodology), 63, 425–464, https://doi.org/10.1111/1467-9868.00294, 2001.

Kleypas, J. A., Mcmanus, J. W., and Meñez, L. A. B.: Environmental Limits to Coral Reef Development: Where Do We Draw the Line?, Am Zool, 39, 146–159, https://doi.org/10.1093/icb/39.1.146, 1999a.

Kleypas, J. A., Mcmanus, J. W., and Meñez, L. A. B.: Environmental Limits to Coral Reef Development: Where Do We Draw the Line?, Am Zool, 39, 146–159, https://doi.org/10.1093/icb/39.1.146, 1999b.

Knutti, R.: The end of model democracy?: An editorial comment, Climatic Change, 102, 395–404, https://doi.org/10.1007/s10584-010-9800-2, 2010.

Kordas, R. L., Harley, C. D. G., and O'Connor, M. I.: Community ecology in a warming world: The influence of temperature on interspecific interactions in marine systems, J. Exp. Mar. Biol. Ecol., 400, 218–226, https://doi.org/10.1016/j.jembe.2011.02.029, 2011.

Kriegler, E., Hall, J. W., Held, H., Dawson, R., and Schellnhuber, H. J.: Imprecise probability assessment of tipping points in the climate system, Proc. Natl. Acad. Sci. U.S.A., 106, 5041–5046, https://doi.org/10.1073/pnas.0809117106, 2009.

Kroeker, K. J., Kordas, R. L., Crim, R. N., and Singh, G. G.: Meta-analysis reveals negative yet variable effects of ocean acidification on marine organisms, Ecology Letters, 13, 1419–1434, https://doi.org/10.1111/j.1461-0248.2010.01518.x, 2010.

Kwiatkowski, L., Torres, O., Bopp, L., Aumont, O., Chamberlain, M., Christian, J. R., Dunne, J. P., Gehlen, M., Ilyina, T., John, J. G., Lenton, A., Li, H., Lovenduski, N. S., Orr, J. C., Palmieri, J., Santana-Falcón, Y., Schwinger, J., Séférian, R., Stock, C. A., Tagliabue, A., Takano, Y., Tjiputra, J., Toyama, K., Tsujino, H., Watanabe, M., Yamamoto, A., Yool, A., and Ziehn, T.: Twenty-first century ocean warming, acidification, deoxygenation, and upper-ocean nutrient and primary production decline from CMIP6 model projections, Biogeosciences, 17, 3439–3470, https://doi.org/10.5194/bg-17-3439-2020, 2020.

Latif, M., Sun, J., Visbeck, M., and Hadi Bordbar, M.: Natural variability has dominated Atlantic Meridional Overturning Circulation since 1900, Nat. Clim. Chang., 12, 455–460, https://doi.org/10.1038/s41558-022-01342-4, 2022.

Lauvset, S. K., Key, R. M., Olsen, A., van Heuven, S., Velo, A., Lin, X., Schirnick, C., Kozyr, A., Tanhua, T., Hoppema, M., Jutterström, S., Steinfeldt, R., Jeansson, E., Ishii, M., Perez, F. F., Suzuki, T., and Watelet, S.: A new global interior ocean mapped climatology: the 1◦ × 1◦ GLODAP version 2, 16, 2016.

Lenton, T. M.: Arctic Climate Tipping Points, AMBIO, 41, 10–22, https://doi.org/10.1007/s13280-011-0221-x, 2012.

Lenton, T. M., Held, H., Kriegler, E., Hall, J. W., Lucht, W., Rahmstorf, S., and Schellnhuber, H. J.: Tipping elements in the Earth's climate system, Proceedings of the National Academy of Sciences, 105, 1786–1793, https://doi.org/10.1073/pnas.0705414105, 2008.

Levermann, A., Clark, P. U., Marzeion, B., Milne, G. A., Pollard, D., Radic, V., and Robinson, A.: The multimillennial sea-level commitment of global warming, Proc. Natl. Acad. Sci. U.S.A., 110, 13745–13750, https://doi.org/10.1073/pnas.1219414110, 2013.

Lienert, S. and Joos, F.: A Bayesian ensemble data assimilation to constrain model parameters and land-use carbon emissions, Biogeosciences, 15, 2909–2930, https://doi.org/10.5194/bg-15-2909-2018, 2018.

Limburg, K. E., Breitburg, D., Swaney, D. P., and Jacinto, G.: Ocean Deoxygenation: A Primer, One Earth, 2, 24–29, https://doi.org/10.1016/j.oneear.2020.01.001, 2020.

Lobelle, D., Beaulieu, C., Livina, V., Sévellec, F., and Frajka-Williams, E.: Detectability of an AMOC Decline in Current and Projected Climate Changes, Geophysical Research Letters, 47, e2020GL089974, https://doi.org/10.1029/2020GL089974, 2020.

Locarnini, R. A., Mishonov, A. V., Antonov, J. I., Boyer, T. P., Garcia, H. E., Baranova, O. K., Zweng, M. M., Paver, C. R., Reagan, J. R., Johnson, D. R., Hamilton, M., Seidov, D., 1948-, and Levitus, S.: World ocean atlas 2013. Volume 1, Temperature, NOAA atlas NESDIS 73, https://doi.org/10.7289/V55X26VD, 2013.

MacDougall, A. H., Swart, N. C., and Knutti, R.: The Uncertainty in the Transient Climate Response to Cumulative CO2 Emissions Arising from the Uncertainty in Physical Climate Parameters, Journal of Climate, 30, 813–827, https://doi.org/10.1175/JCLI-D-16-0205.1, 2017.

Masson-Delmotte, V., Zhai, P., Pirani, A., Connors, S. L., Péan, C., Berger, S., Caud, N., Chen, Y., Goldfarb, L., Gomis, M. I., Huang, M., Leitzell, K., Lonnoy, E., Matthews, J. B. R., Maycock, T. K., Waterfield, T., Yelekçi, O., Yu, R., and Zhou, B. (Eds.): Climate Change 2021: The Physical Science Basis. Contribution of Working Group I to the Sixth Assessment Report of the Intergovernmental Panel on Climate Change, , https://doi.org/10.1017/9781009157896, 2021.

Mckay, M. D., Beckman, R. J., and Conover, W. J.: A Comparison of Three Methods for Selecting Values of Input Variables in the Analysis of Output From a Computer Code, Technometrics, 42, 55–61, https://doi.org/10.1080/00401706.2000.10485979, 2000.

Meissner, K. J., Weaver, A. J., Matthews, H. D., and Cox, P. M.: The role of land surface dynamics in glacial inception: a study with the UVic Earth System Model, Climate Dynamics, 21, 515–537, https://doi.org/10.1007/s00382-003-0352-2, 2003.

Mengis, N., Keller, D. P., MacDougall, A. H., Eby, M., Wright, N., Meissner, K. J., Oschlies, A., Schmittner, A., MacIsaac, A. J., Matthews, H. D., and Zickfeld, K.: Evaluation of the University of Victoria Earth System Climate Model version 2.10 (UVic ESCM 2.10), Geoscientific Model Development, 13, 4183–4204, https://doi.org/10.5194/gmd-13-4183-2020, 2020.

Moore, J. K., Fu, W., Primeau, F., Britten, G. L., Lindsay, K., Long, M., Doney, S. C., Mahowald, N., Hoffman, F., and Randerson, J. T.: Sustained climate warming drives declining marine biological productivity, Science, 359, 1139–1143, https://doi.org/10.1126/science.aao6379, 2018.

Morée, A. L., Clarke, T. M., Cheung, W. W. L., and Frölicher, T. L.: Impact of deoxygenation and warming on global marine species in the 21st century, Biogeosciences, 20, 2425–2454, https://doi.org/10.5194/bg-20-2425-2023, 2023.

Müller, S. A., Joos, F., Edwards, N. R., and Stocker, T. F.: Water Mass Distribution and Ventilation Time Scales in a Cost-Efficient, Three-Dimensional Ocean Model, Journal of Climate, 19, 5479–5499, https://doi.org/10.1175/JCLI3911.1, 2006.

Nash, K. L., Cvitanovic, C., Fulton, E. A., Halpern, B. S., Milner-Gulland, E. J., Watson, R. A., and Blanchard, J. L.: Planetary boundaries for a blue planet, Nat Ecol Evol, 1, 1625–1634, https://doi.org/10.1038/s41559-017-0319-z, 2017.

Nijsse, F. J. M. M., Cox, P. M., and Williamson, M. S.: Emergent constraints on transient climate response (TCR) and equilibrium climate sensitivity (ECS) from historical warming in CMIP5 and CMIP6 models, Earth Syst. Dynam., 11, 737–750, https://doi.org/10.5194/esd-11-737-2020, 2020.

O'Neill, B. C., Tebaldi, C., van Vuuren, D. P., Eyring, V., Friedlingstein, P., Hurtt, G., Knutti, R., Kriegler, E., Lamarque, J.-F., Lowe, J., Meehl, G. A., Moss, R., Riahi, K., and Sanderson, B. M.: The Scenario Model Intercomparison Project (ScenarioMIP) for CMIP6, Geosci. Model Dev., 9, 3461–3482, https://doi.org/10.5194/gmd-9-3461-2016, 2016.

O'Neill, B. C., Oppenheimer, M., Warren, R., Hallegatte, S., Kopp, R. E., Pörtner, H. O., Scholes, R., Birkmann, J., Foden, W., Licker, R., Mach, K. J., Marbaix, P., Mastrandrea, M. D., Price, J., Takahashi, K., Van Ypersele, J.-P., and Yohe, G.: IPCC reasons for concern regarding climate change risks, Nature Clim Change, 7, 28–37, https://doi.org/10.1038/nclimate3179, 2017.

Orr, J. C. and Epitalon, J.-M.: Improved routines to model the ocean carbonate system: mocsy 2.0, Geosci. Model Dev., 8, 485–499, https://doi.org/10.5194/gmd-8-485-2015, 2015.

Orr, J. C., Fabry, V. J., Aumont, O., Bopp, L., Doney, S. C., Feely, R. A., Gnanadesikan, A., Gruber, N., Ishida, A., Joos, F., Key, R. M., Lindsay, K., Maier-Reimer, E., Matear, R., Monfray, P., Mouchet, A., Najjar, R. G., Plattner, G.-K., Rodgers, K. B., Sabine, C. L., Sarmiento, J. L., Schlitzer, R., Slater, R. D., Totterdell, I. J., Weirig, M.-F., Yamanaka, Y., and Yool, A.: Anthropogenic ocean acidification over the twenty-first century and its impact on calcifying organisms, Nature, 437, 681–686, https://doi.org/10.1038/nature04095, 2005.

Pacanowski, R. C. E.: MOM 2. Documentation, User's Guide and Reference Manual. Technical Report 3.2. GFDL Ocean Group, GFDL, Princeton, New Jersey, 1996.

Peng, G., Matthews, J. L., Wang, M., Vose, R., and Sun, L.: What Do Global Climate Models Tell Us about Future Arctic Sea Ice Coverage Changes?, Climate, 8, 15, https://doi.org/10.3390/cli8010015, 2020.

Penn, J. L. and Deutsch, C.: Avoiding ocean mass extinction from climate warming, Science, 376, 524–526, https://doi.org/10.1126/science.abe9039, 2022.

Pereira, H. M., Ferrier, S., Walters, M., Geller, G. N., Jongman, R. H. G., Scholes, R. J., Bruford, M. W., Brummitt, N., Butchart, S. H. M., Cardoso, A. C., Coops, N. C., Dulloo, E., Faith, D. P., Freyhof, J., Gregory, R. D., Heip, C., Höft, R., Hurtt, G., Jetz, W., Karp, D. S., McGeoch, M. A., Obura, D., Onoda, Y., Pettorelli, N., Reyers, B., Sayre, R., Scharlemann, J. P. W., Stuart, S. N., Turak, E., Walpole, M., and Wegmann, M.: Essential Biodiversity Variables, Science, 339, 277–278, https://doi.org/10.1126/science.1229931, 2013.

Pinsky, M. L., Selden, R. L., and Kitchel, Z. J.: Climate-Driven Shifts in Marine Species Ranges: Scaling from Organisms to Communities, Annu. Rev. Mar. Sci., 12, 153–179, https://doi.org/10.1146/annurev-marine-010419-010916, 2020.

Plattner, G.-K., Knutti, R., Joos, F., Stocker, T. F., Von Bloh, W., Brovkin, V., Cameron, D., Driesschaert, E., Dutkiewicz, S., Eby, M., Edwards, N. R., Fichefet, T., Hargreaves, J. C., Jones, C. D., Loutre, M. F., Matthews, H. D., Mouchet, A., Müller, S. A., Nawrath, S., Price, A., Sokolov, A., Strassmann, K. M., and Weaver, A. J.: Long-Term Climate Commitments Projected with Climate–Carbon Cycle Models, Journal of Climate, 21, 2721–2751, https://doi.org/10.1175/2007JCLI1905.1, 2008.

Popova, E. E., Yool, A., Aksenov, Y., Coward, A. C., and Anderson, T. R.: Regional variability of acidification in the Arctic: a sea of contrasts, Biogeosciences, 11, 293–308, https://doi.org/10.5194/bg-11-293-2014, 2014.

Pörtner, H.-O., Roberts, D. C., Masson-Delmotte, V., Zhai, P., Tignor, M. M. B., Poloczanska, E., Mintenbeck, K., Alegría, A., Nicolai, M., Okem, A. E., Petzold, J., Rama, B., and Weyer, N. M. (Eds.): IPCC Special Report on the Ocean and Cryosphere in a Changing Climate, Cambridge University Press, Cambridge, UK and New York, NY, USA, 755 pp., 2019.

Rasmussen, C. E. and Williams, C. K. I.: Gaussian Processes for Machine Learning, The MIT Press, https://doi.org/10.7551/mitpress/3206.001.0001, 2005.

Ritz, S. P., Stocker, T. F., and Joos, F.: A Coupled Dynamical Ocean–Energy Balance Atmosphere Model for Paleoclimate Studies, Journal of Climate, 24, 349–375, 2011.

Rockström, J., Steffen, W., Noone, K., Persson, Å., Chapin, F. S., Lambin, E. F., Lenton, T. M., Scheffer, M., Folke, C., Schellnhuber, H. J., Nykvist, B., De Wit, C. A., Hughes, T., Van Der Leeuw, S., Rodhe, H., Sörlin, S., Snyder, P. K., Costanza, R., Svedin, U., Falkenmark, M., Karlberg, L., Corell, R. W., Fabry, V. J., Hansen, J., Walker, B., Liverman, D., Richardson, K., Crutzen, P., and Foley, J. A.: A safe operating space for humanity, Nature, 461, 472–475, https://doi.org/10.1038/461472a, 2009.

Sacks, J., Welch, W. J., Mitchell, T. J., and Wynn, H. P.: Design and Analysis of Computer Experiments, Statistical Science, 4, 409–423, 1989.

Samanta, A., Anderson, B. T., Ganguly, S., Knyazikhin, Y., Nemani, R. R., and Myneni, R. B.: Physical Climate Response to a Reduction of Anthropogenic Climate Forcing, Earth Interactions, 14, 1–11, https://doi.org/10.1175/2010EI325.1, 2010.

Santana-Falcón, Y., Yamamoto, A., Lenton, A., Jones, C. D., Burger, F. A., John, J. G., Tjiputra, J., Schwinger, J., Kawamiya, M., Frölicher, T. L., Ziehn, T., and Séférian, R.: Irreversible loss in marine ecosystem habitability after a temperature overshoot, Commun Earth Environ, 4, 343, https://doi.org/10.1038/s43247-023-01002-1, 2023.

Schwinger, J., Asaadi, A., Goris, N., and Lee, H.: Possibility for strong northern hemisphere high-latitude cooling under negative emissions, Nat Commun, 13, 1095, https://doi.org/10.1038/s41467-022-28573-5, 2022.

Séférian, R., Nabat, P., Michou, M., Saint-Martin, D., Voldoire, A., Colin, J., Decharme, B., Delire, C., Berthet, S., Chevallier, M., Sénési, S., Franchisteguy, L., Vial, J., Mallet, M., Joetzjer, E., Geoffroy, O., Guérémy, J., Moine, M., Msadek, R., Ribes, A., Rocher, M., Roehrig, R., Salas-y-Mélia, D., Sanchez, E., Terray, L., Valcke, S., Waldman, R., Aumont, O., Bopp, L., Deshayes, J., Éthé, C., and Madec, G.: Evaluation of CNRM Earth System Model, CNRM-ESM2-1: Role of Earth System Processes in Present-Day and Future Climate, J. Adv. Model. Earth Syst., 11, 4182–4227, https://doi.org/10.1029/2019MS001791, 2019.

Seland, Ø., Bentsen, M., Olivié, D., Toniazzo, T., Gjermundsen, A., Graff, L. S., Debernard, J. B., Gupta, A. K., He, Y.-C., Kirkevåg, A., Schwinger, J., Tjiputra, J., Aas, K. S., Bethke, I., Fan, Y., Griesfeller, J., Grini, A., Guo, C., Ilicak, M., Karset, I. H. H., Landgren, O., Liakka, J., Moseid, K. O., Nummelin, A., Spensberger, C., Tang, H., Zhang, Z., Heinze, C., Iversen, T., and Schulz, M.: Overview of the Norwegian Earth System Model (NorESM2) and key climate response of CMIP6 DECK, historical, and scenario simulations, Geosci. Model Dev., 13, 6165–6200, https://doi.org/10.5194/gmd-13-6165-2020, 2020.

Sellar, A. A., Jones, C. G., Mulcahy, J. P., Tang, Y., Yool, A., Wiltshire, A., O'Connor, F. M., Stringer, M., Hill, R., Palmieri, J., Woodward, S., Mora, L., Kuhlbrodt, T., Rumbold, S. T., Kelley, D. I., Ellis, R., Johnson, C. E., Walton, J., Abraham, N. L., Andrews, M. B., Andrews, T., Archibald, A. T., Berthou, S., Burke, E., Blockley, E., Carslaw, K., Dalvi, M., Edwards, J., Folberth, G. A., Gedney, N., Griffiths, P. T., Harper, A. B., Hendry, M. A., Hewitt, A. J., Johnson, B., Jones, A., Jones, C. D., Keeble, J., Liddicoat, S., Morgenstern, O., Parker, R. J., Predoi, V., Robertson, E., Siahaan, A., Smith, R. S., Swaminathan,

R., Woodhouse, M. T., Zeng, G., and Zerroukat, M.: UKESM1: Description and Evaluation of the U.K. Earth System Model, J. Adv. Model. Earth Syst., 11, 4513–4558, https://doi.org/10.1029/2019MS001739, 2019.

Smith, K. E., Burrows, M. T., Hobday, A. J., Sen Gupta, A., Moore, P. J., Thomsen, M., Wernberg, T., and Smale, D. A.: Socioeconomic impacts of marine heatwaves: Global issues and opportunities, Science, 374, eabj3593, https://doi.org/10.1126/science.abj3593, 2021.

Smith, K. E., Sen Gupta, A., Amaya, D., Benthuysen, J. A., Burrows, M. T., Capotondi, A., Filbee-Dexter, K., Frölicher, T. L., Hobday, A. J., Holbrook, N. J., Malan, N., Moore, P. J., Oliver, E. C. J., Richaud, B., Salcedo-Castro, J., Smale, D. A., Thomsen, M., and Wernberg, T.: Baseline matters: Challenges and implications of different marine heatwave baselines, Progress in Oceanography, 231, 103404, https://doi.org/10.1016/j.pocean.2024.103404, 2025.

Steinacher, M. and Joos, F.: Transient Earth system responses to cumulative carbon dioxide emissions: linearities, uncertainties, and probabilities in an observation-constrained model ensemble, Biogeosciences, 13, 1071–1103, https://doi.org/10.5194/bg-13-1071-2016, 2016.

Steinacher, M., Joos, F., Frölicher, T. L., Plattner, G.-K., and Doney, S. C.: Imminent ocean acidification in the Arctic projected with the NCAR global coupled carbon cycle-climate model, Biogeosciences, 6, 515–533, https://doi.org/10.5194/bg-6-515-2009, 2009.

Steinacher, M., Joos, F., and Stocker, T. F.: Allowable carbon emissions lowered by multiple climate targets, Nature, 499, 197–201, https://doi.org/10.1038/nature12269, 2013.

Stroeve, J. C., Kattsov, V., Barrett, A., Serreze, M., Pavlova, T., Holland, M., and Meier, W. N.: Trends in Arctic sea ice extent from CMIP5, CMIP3 and observations, Geophys. Res. Lett., 39, 2012GL052676, https://doi.org/10.1029/2012GL052676, 2012.

Swart, N. C., Cole, J. N. S., Kharin, V. V., Lazare, M., Scinocca, J. F., Gillett, N. P., Anstey, J., Arora, V., Christian, J. R., Hanna, S., Jiao, Y., Lee, W. G., Majaess, F., Saenko, O. A., Seiler, C., Seinen, C., Shao, A., Sigmond, M., Solheim, L., von Salzen, K., Yang, D., and Winter, B.: The Canadian Earth System Model version 5 (CanESM5.0.3), Geosci. Model Dev., 12, 4823–4873, https://doi.org/10.5194/gmd-12-4823-2019, 2019.

Tagliabue, A., Kwiatkowski, L., Bopp, L., Butenschön, M., Cheung, W., Lengaigne, M., and Vialard, J.: Persistent Uncertainties in Ocean Net Primary Production Climate Change Projections at Regional Scales Raise Challenges for Assessing Impacts on Ecosystem Services, Front. Clim., 3, 738224, https://doi.org/10.3389/fclim.2021.738224, 2021.

Terhaar, J., Kwiatkowski, L., and Bopp, L.: Emergent constraint on Arctic Ocean acidification in the twenty-first century, Nature, 582, 379–383, https://doi.org/10.1038/s41586-020-2360-3, 2020.

Terhaar, J., Torres, O., Bourgeois, T., and Kwiatkowski, L.: Arctic Ocean acidification over the 21st century co-driven by anthropogenic carbon increases and freshening in the CMIP6 model ensemble, Biogeosciences, 18, 2221–2240, https://doi.org/10.5194/bg-18-2221-2021, 2021.

Terhaar, J., Frölicher, T. L., and Joos, F.: Ocean acidification in emission-driven temperature stabilization scenarios: the role of TCRE and non-CO_2 greenhouse gases, Environ. Res. Lett., 18, 024033, https://doi.org/10.1088/1748-9326/acaf91, 2023.

Terhaar, J., Vogt, L., and Foukal, N. P.: Atlantic overturning inferred from air-sea heat fluxes indicates no decline since the 1960s, Nat Commun, 16, 222, https://doi.org/10.1038/s41467-024-55297-5, 2025.

Tittensor, D. P., Novaglio, C., Harrison, C. S., Heneghan, R. F., Barrier, N., Bianchi, D., Bopp, L., Bryndum-Buchholz, A., Britten, G. L., Büchner, M., Cheung, W. W. L., Christensen, V., Coll, M., Dunne, J. P., Eddy, T. D., Everett, J. D., Fernandes-Salvador, J. A., Fulton, E. A., Galbraith, E. D., Gascuel, D., Guiet, J., John, J. G., Link, J. S., Lotze, H. K., Maury, O., Ortega-Cisneros, K., Palacios-Abrantes, J., Petrik, C. M., du Pontavice, H., Rault, J., Richardson, A. J., Shannon, L., Shin, Y.-J., Steenbeek, J., Stock, C. A., and Blanchard, J. L.: Next-generation ensemble projections reveal higher climate risks for marine ecosystems, Nat. Clim. Chang., 11, 973–981, https://doi.org/10.1038/s41558-021-01173-9, 2021.

Tokarska, K. B., Zickfeld, K., and Rogelj, J.: Path Independence of Carbon Budgets When Meeting a Stringent Global Mean Temperature Target After an Overshoot, Earth's Future, 7, 1283–1295, https://doi.org/10.1029/2019EF001312, 2019.

Tokarska, K. B., Stolpe, M. B., Sippel, S., Fischer, E. M., Smith, C. J., Lehner, F., and Knutti, R.: Past warming trend constrains future warming in CMIP6 models, Sci. Adv., 6, eaaz9549, https://doi.org/10.1126/sciadv.aaz9549, 2020.

UNFCCC: Adoption of the Paris Agreement, Report No. FCCC/CP/2015/L.9/Rev.1, 2015.

Van Gennip, S. J., Popova, E. E., Yool, A., Pecl, G. T., Hobday, A. J., and Sorte, C. J. B.: Going with the flow: the role of ocean circulation in global marine ecosystems under a changing climate, Glob. Chang. Biol., 23, 2602–2617, https://doi.org/10.1111/gcb.13586, 2017.

Van Westen, R. M., Kliphuis, M., and Dijkstra, H. A.: Physics-based early warning signal shows that AMOC is on tipping course, Sci. Adv., 10, eadk1189, https://doi.org/10.1126/sciadv.adk1189, 2024.

Vaquer-Sunyer, R. and Duarte, C. M.: Thresholds of hypoxia for marine biodiversity, Proc. Natl. Acad. Sci. U.S.A., 105, 15452–15457, https://doi.org/10.1073/pnas.0803833105, 2008.

Waldbusser, G. G., Hales, B., Langdon, C. J., Haley, B. A., Schrader, P., Brunner, E. L., Gray, M. W., Miller, C. A., and Gimenez, I.: Saturation-state sensitivity of marine bivalve larvae to ocean acidification, Nature Clim Change, 5, 273–280, https://doi.org/10.1038/nclimate2479, 2015.

WCRP Global Sea Level Budget Group: Global sea-level budget 1993–present, Earth Syst. Sci. Data, 10, 1551–1590, https://doi.org/10.5194/essd-10-1551-2018, 2018.

Weaver, A. J., Eby, M., Wiebe, E. C., Bitz, C. M., Duffy, P. B., Ewen, T. L., Fanning, A. F., Holland, M. M., MacFadyen, A., Matthews, H. D., Meissner, K. J., Saenko, O., Schmittner, A., Wang, H., and Yoshimori, M.: The UVic earth system climate model: Model description, climatology, and applications to past, present and future climates, Atmosphere-Ocean, 39, 361–428, https://doi.org/10.1080/07055900.2001.9649686, 2001.

Weaver, A. J., Sedláček, J., Eby, M., Alexander, K., Crespin, E., Fichefet, T., Philippon-Berthier, G., Joos, F., Kawamiya, M., Matsumoto, K., Steinacher, M., Tachiiri, K., Tokos, K., Yoshimori, M., and Zickfeld, K.: Stability of the Atlantic meridional overturning circulation: A model intercomparison, Geophys. Res. Lett., 39, 2012GL053763, https://doi.org/10.1029/2012GL053763, 2012.

Weijer, W., Cheng, W., Garuba, O. A., Hu, A., and Nadiga, B. T.: CMIP6 Models Predict Significant 21st Century Decline of the Atlantic Meridional Overturning Circulation, Geophys. Res. Lett., 47, e2019GL086075, https://doi.org/10.1029/2019GL086075, 2020.

Williamson, D., Blaker, A. T., Hampton, C., and Salter, J.: Identifying and removing structural biases in climate models with history matching, Clim Dyn, 45, 1299–1324, https://doi.org/10.1007/s00382-014-2378-z, 2015.

Williamson, P. and Guinder, V. A.: Effect of climate change on marine ecosystems, in: The Impacts of Climate Change, Elsevier, 115–176, https://doi.org/10.1016/B978-0-12-822373-4.00024-0, 2021.

Yamamoto-Kawai, M., McLaughlin, F. A., Carmack, E. C., Nishino, S., and Shimada, K.: Aragonite Undersaturation in the Arctic Ocean: Effects of Ocean Acidification and Sea Ice Melt, Science, 326, 1098–1100, https://doi.org/10.1126/science.1174190, 2009.

Zickfeld, K., Levermann, A., Morgan, M. G., Kuhlbrodt, T., Rahmstorf, S., and Keith, D. W.: Expert judgements on the response of the Atlantic meridional overturning circulation to climate change, Climatic Change, 82, 235–265, https://doi.org/10.1007/s10584-007-9246-3, 2007.

Ziehn, T., Chamberlain, M. A., Law, R. M., Lenton, A., Bodman, R. W., Dix, M., Stevens, L., Wang, Y.-P., and Srbinovsky, J.: The Australian Earth System Model: ACCESS-ESM1.5, JSHESS, 70, 193, https://doi.org/10.1071/ES19035, 2020.

Zweng, M. M., Reagan, J. R., Antonov, J. I., Locarnini, R. A., Mishonov, A. V., Boyer, T. P., Garcia, H. E., Baranova, O. K., Johnson, D. R., Seidov, D., 1948-, Biddle, M. M., and Levitus, S.: World ocean atlas 2013. Volume 2, Salinity, NOAA Atlas NESDIS 74, https://doi.org/10.7289/V5251G4D, 2013.